Appendix P

Climate Change

CLIMATE CHANGE

This chapter is intended to provide background information and context of climate change science as it pertains to the DRECP landscape. It describes some of the climate-related analyses intended to inform the DRECP as implemented in the overall adaptive management framework.

Climate Setting of the DRECP Region

Mojave and Sonoran deserts in the DRECP region occupy the lowest elevations on the eastern slopes of the southern Sierra Nevada and the mountains of southern California, below sea level in the Salton Sea Basin and the Death Valley region, upward to 1,500m along the Sierra Nevada (Figure 1). The desert is fairly continuous and only punctuated by scattered mountains and plateaus, particularly in the Mojave portion of the region and along the western fringe where grasslands, woodlands, or forests can occur.

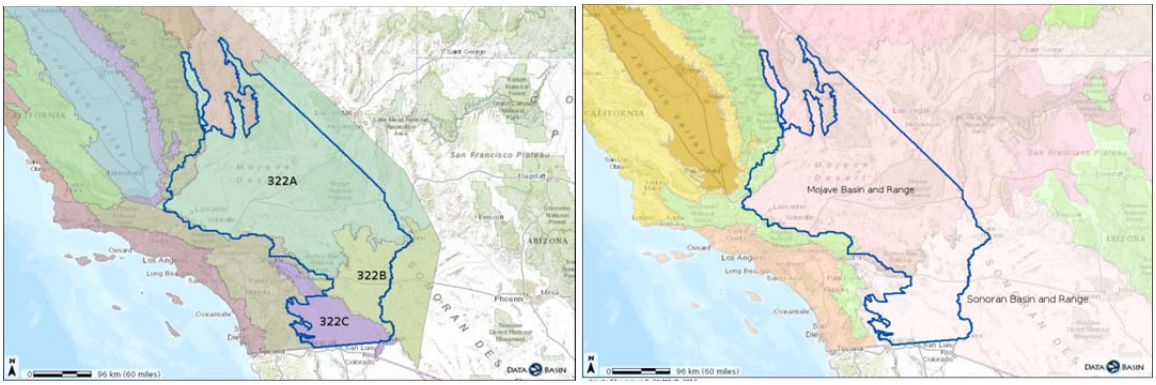

Figure 1. Omernik (1987)'s ecoregions in the DRECP region (Left) [322A= Mojave Desert Section; 322B= Sonoran Desert Section; 322C= Colorado Desert Section in the American Semi-Desert and Desert Province] and Bailey (1983)'s ecoregions in the project area (right).

Southwest US deserts are characterized by warm temperatures (Figure 2), but the Mojave is a high desert with elevations between 600 and 1,200m, consequently with lower minimum temperatures. The Mojave Desert is generally an area of extreme temperatures with a mean July maximum of 47°C (117°F) in Death Valley – one of the hottest places on earth. The Sonoran desert is the hottest North American desert in part because of its low elevation (<600m). Annual frost-free season ranges from 210 to 365 days in Mojave and Sonoran Deserts, respectively.

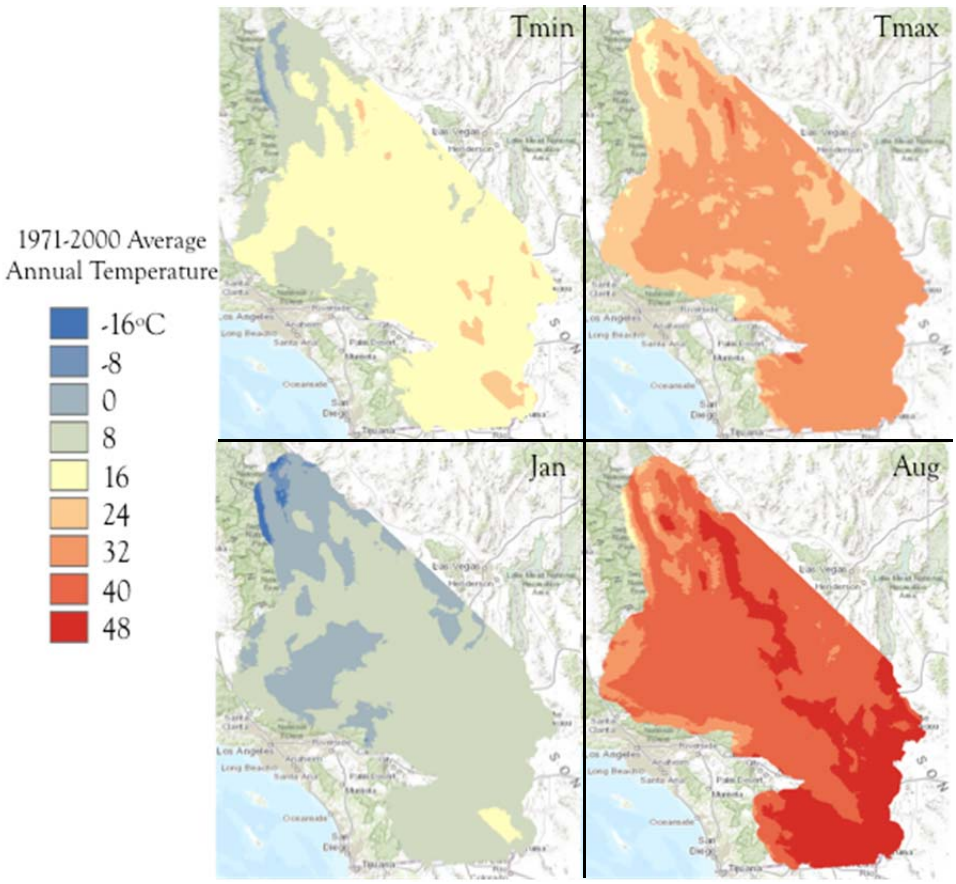

Figure 2. Mean annual minimum (T_{min}) and maximum temperature (T_{max}) (top row), minimum January temperature and maximum August temperature (bottom row), for the DRECP region based on Flint and Flint (2012) climate data at 270m resolution (derived from PRISM 4km).

North American deserts are thought to be semi-deserts rather than true deserts because of their relatively lush vegetation (McMahon 2000). However, some sites are equal in aridity to deserts elsewhere in the world. For example, Furnace Creek in Death Valley has a long term mean rainfall of 42 mm y^{-1} and in 1929 and 1954 there was no rainfall at all over 12 month (Hunt 1975). In general, precipitation is low in amount and highly variable from year to year.

Seasonal rainfall patterns vary significantly over the DRECP region. The Mojave Desert portion of the landscape receives primarily winter rainfall (spring growing season), but a majority of the Sonoran Desert has a bimodal rainfall regime (spring and summer growing seasons) driven by the Arizona summer monsoon (Figure 3). This distinction in seasonal rainfall is sufficient to cause significant differences in vegetation structure and floristic composition. MacMahon (2000) illustrated this by plotting his and others' study sites across temperature and precipitation gradients (Figure 4). The ecotone

between these two desert systems, well represented in the DRECP region, is known for its species and genetic diversity (Wood et al. 2012).

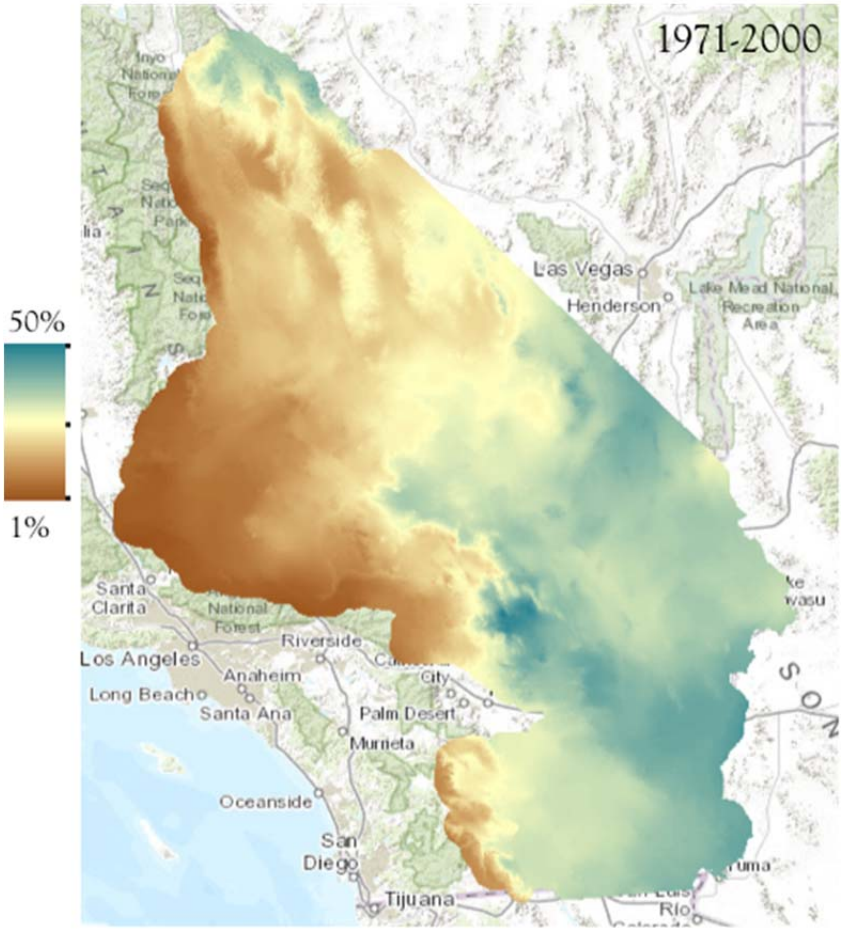

Figure 3. Proportion of annual rainfall occurring during summer months in the DRECP area. The area affected by the summer monsoon is clearly visible in shades of blue.

During winter, storms originating in the Pacific Ocean move inland and are pushed against the Coast Ranges or the Sierra Nevada mountains. This causes adiabatic cooling, condensation, and long-duration low-intensity rainfall over large areas. As storm tracks move north, strong storm cells from the Gulf of Mexico (the Arizona monsoon) move northwestward causing cyclonic thunderstorms of short duration and high intensity limited in areal extent (MacMahon 2000). While mountain ranges create rain shadows, the Sierra Nevada for the Mojave Desert and the Peninsular Ranges for the Sonoran Desert, it is a stable high pressure Hadley cell over the area that, historically, has caused the Sonoran aridity.

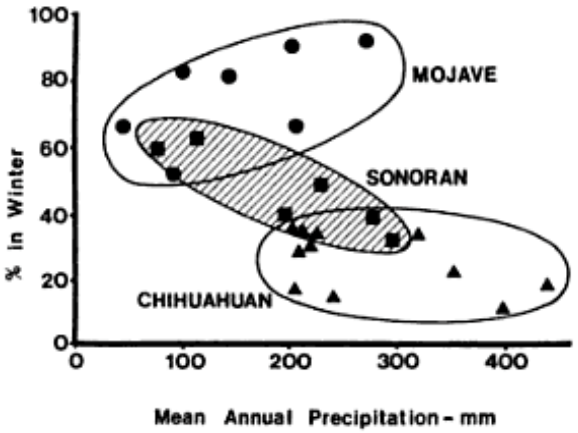

Figure 4. Percentage of winter rainfall plotted against mean annual precipitation for a variety of sites. Adapted from MacMahon and Wagner (1985) and cited in MacMahon (2000).

Flint and Flint (2012) conducted a detailed analysis of the water budget in California. Their map of actual evapotranspiration (AET) displays the variations in drought conditions across the DRECP region, and the difference between potential evapotranspiration (PET) and AET highlights areas where evaporative demand is greater than the available water (Figure 5).

Recent studies have shown that climate change has already affected southern California where regional increases in temperature (LaDochy et al. 2007) and vegetation shifts (Guida 2011, Kelley and Goulden 2008) have been observed. Guida (2011) observed over the last 30 years (1979-2008) an increase of 1.5° C in the average annual minimum temperature and a decrease of 3cm in the average annual precipitation in the Newberry Mountains, on the southeastern corner of the Mojave Desert transitioning to Sonoran conditions. Changes were more pronounced at high elevation and Guida (2011) concluded from his correlations between climate and species distributions that those species that relied the most on higher precipitation levels were likely already migrating to higher elevations in order to adapt to the on-going changes in climate. Similarly, Kelly and Goulden (2008) attributed to climate change the shifts in vegetation distribution they observed along the Deep Canyon Transect of Southern California's Santa Rosa Mountains between 1977 and 2007. While they associated mortality events to two extreme drought periods, they documented the upslope movement of the dominant species by approximately 60m in 30 years and linked it to the increase in climate variability (particularly precipitation) and warming.

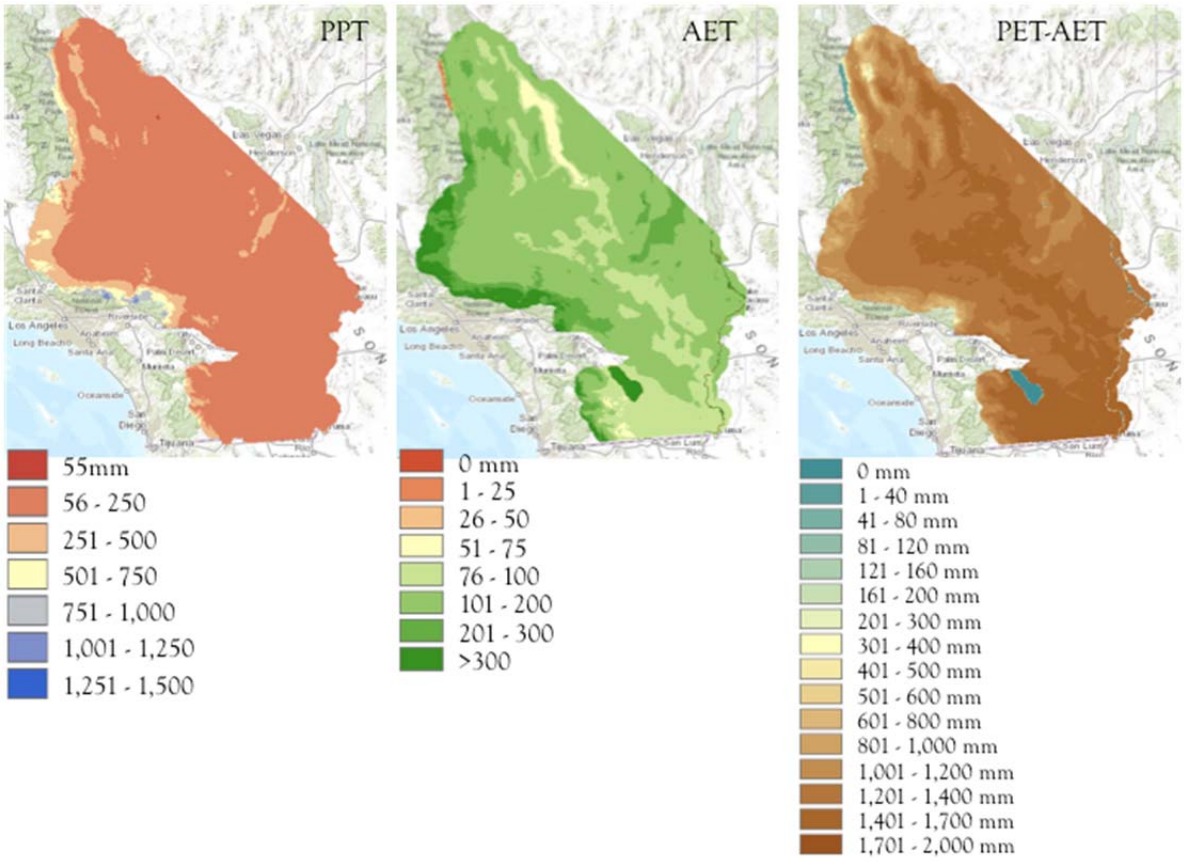

Figure 5. Mean annual precipitation (PPT), actual evapotranspiration (AET), and climate water deficit (PET-AET) for the period 1971-2000 at 270m resolution (Flint and Flint 2012).

Background on Climate Change Models and Emission Scenarios

Climate Change Models

Climate modeling has been conducted by numerous research facilities from around the world for many decades and the level of modeling sophistication has grown over this time. The international body of climate modeling work along with additional socio-economic analyses is routinely summarized by the Intergovernmental Panel on Climate Change (IPCC) and distributed to the world through periodic Assessment Reports (ARs). General Circulation Models (GCMs), which are also referred to as Global Climate Models by the media and the general public, are the most common types of climate models. GCMs were designed to simulate the earth's climate using a coarse resolution

of several hundreds of kilometers for each of their grid cells; the size of which was related to the computer power available when they were first developed. Efforts to refine GCMs have been ongoing for at least four decades. The first GCM that combined both oceanic and atmospheric processes (AOGCM) was developed in the late 1960s. Two figures extracted from the AR4 IPCC report (2007) graphically explain the evolution from the First IPCC Report (FAR) to the 4th (AR4) in terms of spatial resolution and complexity in representing earth system processes (Figure 6).

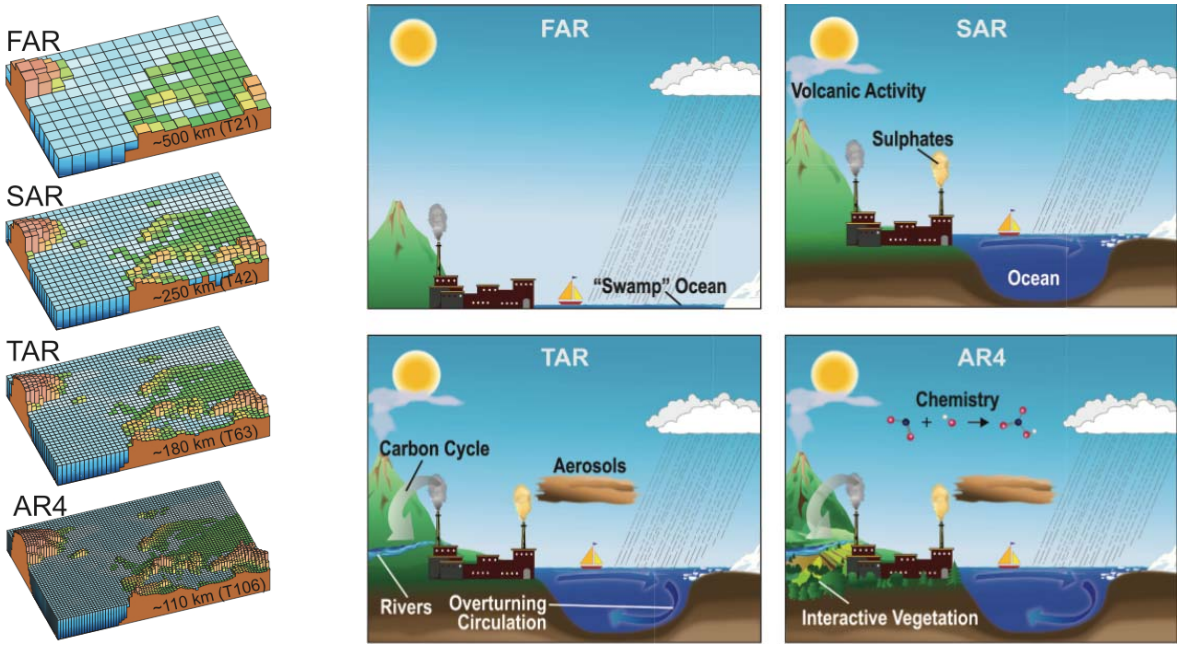

Figure 6. Evolution of the spatial resolution (left) and complexity in process representation (right) of the GCMs from the first (FAR) to the 4th (AR4) Assessment Report for the IPCC (Figures extracted from Alley et al. 2007).

For the IPCC AR4 report published in 2007, climate modelers provided a suite of future climates that were documented, compared, and made publically available through the Phase 3 Coupled Model Inter-comparison Project (CMIP3) web portal. The climate models were developed by 17 different modeling teams from around the world using a variety of spatial resolutions for both atmosphere and ocean representations (Table 1). Each acronym corresponds to a particular version of a GCM model from a specific modeling team. For example, BCC-CM1 is version 1 of a model created in 2005 by the Beijing Climate Center, part of China Meteorological Administration. Please note that

some models have been used since the late 1990s while others have been developed in the following decade.

Table 1. List of CMIP3 climate models simplified from Randall et al. (2007).

GCM (general circulation model	Vintage and source	Atmosphere resolution Grid cell size degree Lat x Long L: # vertical levels	Ocean resolution Grid cell size degree Lat x Long L: # vertical levels
BCC-CM1	2005 Beijing Climate Center (China)	1.9x1.9 L16	1.9x1.9 L30
BCCR-BCM2.0	2005 Bjerknes Center for Climate Research (Norway)	1.9x1.9 L31	0.5-1.5x1.5 L35
CCSM3	2005 NCAR (USA)	1.4x1.4 L26	0.3-1.0x1.0 L40
CGCM3.1 (T47)	2005 Canadian Center for Climate Modeling and Analysis (Canada)	~2.8x2.8 L31	1.9x1.9 L29
CGCM3.1 (T63)	2005 Canadian Center for Climate Modeling and Analysis (Canada)	~2.8x2.8 L31	0.9x1.4 L29
CNRM-CM3	2004 Meteo France and CNRS (France)	~1.9x1.9 L45	0.5-2.0x2.0 L31
CSIRO-MK3.0	2001 Commonwealth Scientific and Industrial Research Organization Atmospheric Research (Australia)	~1.9x1.9 L18	0.8x1.9 L31
ECHAM5/MPI-OM	2005 Max Planck Institute for Meteorology (Germany)	~1.9x1.9 L31	1.5x1.5 L40
ECHO-G	1999 Meteorological Institute of the University of Bonn, Meteorological Research Institute of the Korea Meteorological Administration and Model and Data Group (Germany and Korea)	~3.9x3.9 L19	0.5-2.8x2.8 L20
FGOALS-g1.0	2004 National Key Laboratory of Numerical Modeling for Atmospheric Sciences and Geophysical Fluid Dynamics and Institute of Atmospheric Physics (China)	~2.8x2.8	1.0x1.0 L16
GFDL-CM2.0	2005 US Dept of Commerce and NOAA/GFDL (USA)	2.0x2.5 L24	0.3-1.0x1.0
GFDL-CM2.1	2005 US Dept of Commerce	2.0x2.5	0.3-1.0x1.0

	and NOAA/GFDL (USA)	L24	
GISS-AOM	2004 NASA-Goddard Institute for Space Studies (GISS) (USA)	3.0x4.0 L12	3.0x4.0 L16
GISS-EH	2004 NASA-GISS (USA)	4.0x5.0 L20	2.0x2.0 L16
GISS-ER	2004 NASA-GISS (USA)	4.0x5.0 L20	4.0x5.0 L13
INM-CM3.0 2004	2004 Institute for Numerical Mathematics (Russia)	4.0x5.0 L21	2.0x2.5 L33
IPSL-CM4	2005 Institut Pierre Simon Laplace (France)	2.5x3.75 L19	2.0x2.0 L31
MIROC3.2 (hires)	2004 Center for Climate System Research (U. Tokyo), National Institute of Environmental Studies, and Frontiers Research Center for Global Change (Japan)	~1.1x1.1 L56	0.2x0.3 L47
MIROC3.2 (medres)	2004 Center for Climate System Research (U. Tokyo), National Institute of Environmental Studies, and Frontiers Research Center for Global Change (Japan)	~2.8x2.8 L20	0.5-1.4x1.4 L43
MRI-CGCM2.3.2	2003 Meteorological Research Institute (Japan)	~2.8x2.8 L30	0.5-2.0x2.5 L23
PCM	1998 NCAR (USA)	~2.8x2.8 L26	0.5-0.7x1.1 L40
UKMO-HadCM3	1997 Hadley Center for Climate Prediction and Research/Met Office (UK)	2.5x3.75 L19	1.25x1.25 L20
UKMO-HadGEM1	2004 Hadley Center for Climate Prediction and Research/Met Office (UK)	~1.3x1.9 L38	0.3-1.0x1.0 L40

The 5th assessment report (AR5) for the IPCC, which was released in September 2013, featured a set of results from old and new climate models that have started to be used by a variety of impact models (Table 2). Since the last IPCC report (2007), Earth System Models (ESMs) have been introduced as an attempt to add more details (e.g. nitrogen cycle, dynamic vegetation, fire emissions) to the representation of the biosphere in climate models. All climate models (GCMs or ESMs) can be ranked to reflect their ability to simulate current conditions. However, there is no certainty that a single model that can hindcast the past accurately can also project the future with high reliability.

There has been an increasing interest in Regional Climate Models (RCMs), which use

GCM results as boundary conditions to simulate local climate conditions at finer spatial resolutions. RCMs are becoming more popular especially in places where regional atmospheric processes might be locally decoupled from global climate patterns. Results from one RCM (RegCM3) have been generated for the DRECP region via Regional Ecoregional Assessment (REA) work funded by BLM (gain access to final reports and spatial data for the Sonoran and Mojave Basin and Range from http://www.blm.gov/wo/st/en/prog/more/Landscape_Approach/reas.html).

Table 2. List of CMIP5 climate models from Rupp et al. (2013). The three models highlighted in yellow were chosen for this study since they bracket a wide range of precipitation projections in the DRECP area.

GCM (general circulation model) or ESM (Earth System Model)	**Origin**	**Atmosphere resolution Gridcell size degree Lat x Lon L: # vertical levels**
BCC-CSM1-1	Beijing Climate Center, China Meteorological Administration	2.8x2.8 L26
BCC-CSM1-1-M	Beijing Climate Center, China Meteorological Administration	1.12x1.12 L26
BNU-ESM	College of global change and earth system science, Beijing Normal University, China	2.8x1.4 L26
CanESM2	Canadian Center for Climate Modelling and Analysis (Canada)	2.8x2.8 L35
CCSM4	NCAR (USA)	1.25x.94 L26
CESM1-BGC	Community earth system model contributors	1.25x.94 L26
CESM1-CAM5	Community earth system model contributors	1.25x.94 L26
CESM1-FASTCHEM	Community earth system model contributors	1.25x.94 L26
CESM1-WACCM	Community earth system model contributors	2.5x.1.89 L26
CMCC-CESM	Centro Euro-Mediterraneo per I Cambiamenti Climatici	3.75x3.71 L39
CMCC-CM	Centro Euro-Mediterraneo per I Cambiamenti Climatici	.75x.75
CNRM-CM5	Meteo France and CNRS (France)	1.4x1.4 L31
CSIRO-MK3-6.0	Commonwealth Scientific and Industrial Research Organization, Queensland Climate Change Center of Excellence (Australia)	1.8x1.8 L18
EC-EARTH	EC-EARTH consortium	1.13x1.12

		L62
FGOALS-s2	National Key Laboratory of Numerical Modelling for Atmospheric Sciences and Geophysical Fluid Dynamics and Institute of Atmospheric Physics, Chinese Academy of Sciences (China)	2.8x21.6 L26
FIO-ESM	First Institute of Oceanography	2.81x2.79 L26
GFDL-CM2pl	NOAA/GFDL (USA)	2.5x2.0 L24
GFDL-CM3	NOAA/GFDL (USA)	2.5x2.0 L48
GFDL-ESM2G	NOAA/GFDL (USA)	2.5x2.0 L48
GFDL-ESM2M	NOAA/GFDL (USA)	2.5x2.0 L48
GISS-E2-H	NASA-Goddard Institute for Space Studies (USA)	2.5x2.0 L40
GISS-E2-R	NASA-GISS (USA)	2.5x2.0 L40
HadCM3	Meteorological Office Hadley Center, UK	3.75x2.5 L19
HadGEM2-AO	Meteorological Office Hadley Center, UK	1.88x1.25 L38
HadGEM2-CC	Meteorological Office Hadley Center, UK	1.88x1.25 L60
HadGEM2-ES	Meteorological Office Hadley Center, UK	1.88x1.25 L38
INM-CM4	Institute for Numerical Mathematics (Russia)	2.0x1.5 L21
IPSL-CM5A-LR	Institut Pierre Simon Laplace (France)	3.75x1.8 L39
IPSL-CM5A-MR	Institut Pierre Simon Laplace (France)	2.5x1.25 L39
MIROC5	Atmosphere and Ocean Research Institute (U. Tokyo), National Institute for Environmental Studies, Japan Agency for Marine-Earth Science and Technology (Japan)	1.4x1.4 L40
MIROC-ESM	Atmosphere and Ocean Research Institute (U. Tokyo), National Institute for Environmental Studies, Agency for Marine-Earth Science and Technology (Japan)	2.8x2.8 L80
MIROC-ESM-CHEM	Atmosphere and Ocean Research Institute (U. Tokyo), National Institute for Environmental Studies, Agency for Marine-Earth Science and Technology (Japan)	2.8x2.8 L80
MPI-ESM-LR	Max Planck Institute for Meteorology (Germany)	1.88x1.87 L47
MPI-ESM-MR	Max Planck Institute for Meteorology (Germany)	1.88x1.87 L95
MRI-CGCM3	Meteorological Research Institute (Japan)	1.1x1.1 L48

NorESM1-M	Norwegian Climate Center	2.5x1.9 L26
NorESM1-ME	Norwegian Climate Center	2.5x1.9 L26

Emission Scenarios

Climate models are designed to forecast future climate conditions based on different scenarios informed by economic trajectories, human population trends, governance, and technology advancements over the modeling time frame. Until the most recent IPCC report (2013), emission scenarios were essentially different storylines with a set of assumptions, which each climate model would test in order to evaluate the resulting future climate (Figure 7). The scenarios described in the Special Report on Emission Scenarios (SRES) for the IPCC 4th Assessment Report (AR4), ranged from a business as usual response (A2) to an aggressive response to climate change by the international community (B1). Like climate models, the storyline scenarios had their own acronyms and specific descriptions (i.e., A1Fi, A1T, A1B, A2, B1, and B2).

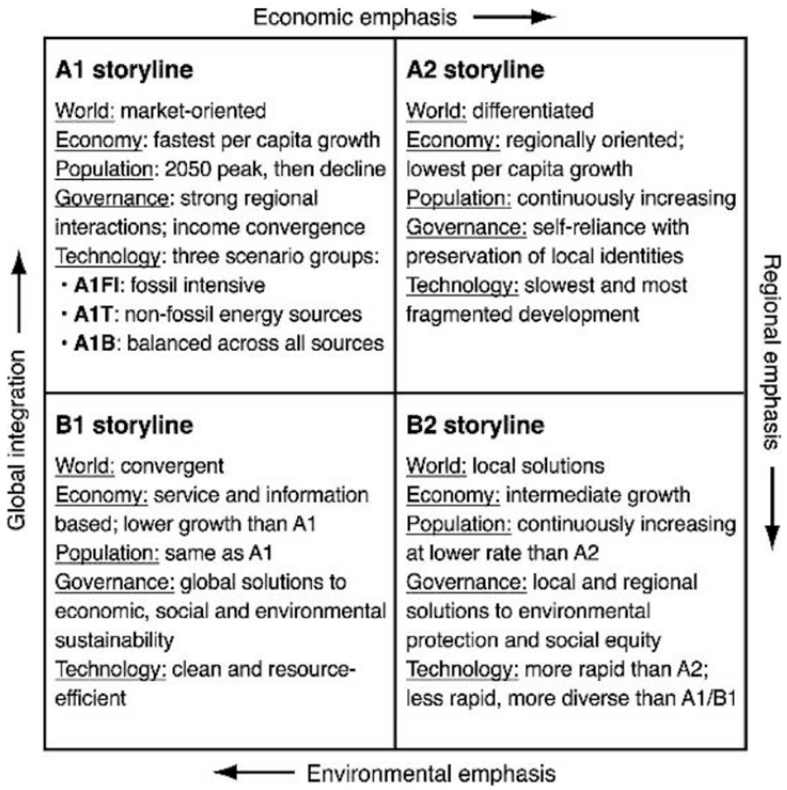

Figure 7. Brief summary of the four Special Report on Emission Scenarios (SRES) storylines (from Parry et al. 2007, fig. TS.2).

In the latest IPCC AR5 (2013), the storyline scenarios have been replaced by four Representative Concentration Pathways (RCPs), developed by four different modeling teams, projecting the evolution of the concentration of atmospheric carbon dioxide over time. Even though each scenario approach covers a wide range of possibilities, neither the SRES developed for AR4 nor the RCPs developed for the AR5 cover the full range of potential futures (Hayhoe, pers. comm. 2012). While the SRES scenarios were developed by one modeling team as a group of socioeconomic storylines associated with global population projections (Nakicenovic et al. 2000) without any climate policy considerations, the RCPs (VanVuuren et al. 2011) were developed to simulate for the end of the 21st century four levels of radiative forcing (8.5 Wm^{-2} to 2.6 W m^{-2} by 2100) resulting from different carbon dioxide concentration trajectories driven by diverse climate policies. There are similarities between the climate futures generated under SRES and RCP scenarios but also differences mostly due to the higher level of complexity in the climate models (Table 3). For example under RCP scenarios, the upper limit of sea level rise has increased due to more attention paid to ice sheet melting. Note also that the lower limits of the temperature range reached at the end of the 21st century are higher under RCPs than under SRES scenarios but the higher limits are somewhat lower. It is important to note that while RCPs have been widely accepted and used by the scientific community, climate change impacts continue to be evaluated with the more consistent SRES storylines such as the most recent US National Climate Assessment (2014).

Table 3. Comparison between SRES (Special Report on Emission Scenarios) and RCP (Representative Concentration Pathways) emission scenarios based on Rogelj et al. (2012) who provided probabilistic estimates of temperature increase above pre-industrial levels in a consistent framework to compare climate projections. Note that the time periods were chosen to accommodate for some of the CMIP5 models like the Hadley series which stops in 2099 instead of 2100. Consequently the historical baseline was chosen by the authors to match the last 20 years of the 21st century.

Emission Scenarios	**Atmospheric CO_2 concentration in 2100 (ppm)**	**Temperature change in ^oC 2090-99 relative to 1980-99 (median value in parenthesis)**	**Global Mean Sea Level Rise (m) at 2090-99 relative to 1980-99 (Source Alley et al. 2007 and Jevrejeva et al. 2012)**
SRES A1Fi	958	2.4-6.4 (4.0)	0.26-0.59
RCP 8.5	936	3.8-5.7 (4.6)	0.81-1.65
SRES A2	846	2.0-5.4 (3.4)	0.23-0.51
SRES A1B	703	1.7-4.4 (2.8)	0.21-0.48
RCP 6.0	670	2.5-3.6 (2.9)	0.6-1.26
SRES B2	611	1.4-3.8 (2.4)	0.2-0.43

SRES A1T	575	1.4-3.8 (2.4)	0.20-0.45
SRES B1	544	1.1-2.9 (1.8)	0.18-0.38
RCP 4.5	538	2.0-2.9 (2.4)	.52-1.10
RCP 2.6	421	1.3-1.9 (1.5)	.36-.83

Climate Projections for the DRECP Region

Temperature – AR4

North American deserts are expected to become warmer at faster rates than other regions (Stahlschmidt et al. 2011). Climate projections from various sources (Table 4) agree that temperatures will increase in the southern California deserts by more than 2°C (Stralberg et al. 2009, Snyder and Sloan 2005, Snyder et al. 2004, Bell et al. 2004) while observations are already showing a measurable warming that has occurred during the last 30 years (LaDochy et al. 2007).

Table 4. Summary of published projections of temperature change in the southern California deserts from various sources (as cited by PRBO 2011 - now called Point Blue Conservation Science).

Climate Variable	Mojave	Sonoran	Reference	GCM/RCMs
Mean annual temperature difference	1.9-2.6°C ([2038-70 ave] - [1970-99 ave])	1.8-2.4 °C ([2038-70 ave] - [1970-99 ave])	Stralberg et al. 2009 cited in PRBO 2011	RegCM3-CCSM3.0 & GFDL CM2.1 A2
	2.8°C [2xCO_2] (1980-99 vs 2080-99)	2.7°C	Snyder and Sloan 2005	RegCM2.5-CSM1.2
Monthly median temperature difference	2.2°C (>2°C except Oct-Nov)	2.1°C (>2°C except Jan, Jul, Oct-Dec)	Snyder et al. 2004	RegCM2.5-CCM3
Mean diurnal temperature range difference	0-0.2°C ([2038-70 ave] - [1970-99 ave])	0-0.2°C	Stralberg et al. 2009 cited in PRBO 2011	RegCM3-CCSM 3.2 & GFDL CM2.1 A2
	-0.3°C (2080-99)	-0.1°C (2080-99)	Snyder and Loan 2005	RegCM2.5-CCM3
	0.18°C [2xCO_2]	0.07°C	Bell et al. 2004	RegCM2.5-CCM3
Tmin/max	2.6/2.4°C [2xCO_2]	2.3/2.2°C [2xCO_2]	Bell et al. 2004	RegCM2.5-CCM3
#hot days/#>32.2°	+31/+27 days per year	+22/+20 days per year	Bell et al. 2004	RegCM2.5-CCM3

C				
>=7 day hot spells	+1.1 events/yr 10 days longer +0.6°C	+1.0 event/yr 6 days longer +0.8°C	Bell et al. 2004	RegCM2.5-CCM3
# extreme cold days/#<0°C	-43/-38 days per year	-44/-10 days per year	Bell et al. 2004	RegCM2.5-CCM3
>=7 day cold spells	-1.9 events 3.8 fewer days +0.4°C	-1.3 events 4.3 fewer days +0.2°C	Bell et al. 2004	RegCM2.5-CCM3
DD >0°C (frost free growing season)	22 days earlier 31 days longer	22 days earlier 30 days longer	Bell et al. 2004	RegCM2.5-CCM3

Based on Cayan et al. (2008) recommendations, Flint and Flint (2012) selected two climate change scenarios from the IPCC Fourth Assessment (2007) – PCM and GFDL to examine potential futures for California. The projections were required to contain realistic representations of regional climatic features, such as the summer monsoon, with a spatiotemporal variability that could reproduce recent historical climate in California as well as exhibit different levels of sensitivity to greenhouse gas forcing.

We present summary results of these model projections using the climate data provided by the California Climate Commons for the A2 emission scenario only. In general, the GFDL model simulates warmer conditions than PCM, but in both cases projections show that the warming will be extensive across the entire DRECP region. For example, while the current area exposed to an average annual Tmax of 40°C is small, it is projected to expand and cover at least a third of the region under both sets of climate projections by the end of the century (Figure 8). Mean annual minimum temperatures are also expected to increase considerably, especially in the GFDL projections (Figure 9). Historic records of minimum temperatures from PRISM (Figure 10) have already shown a significant increase in temperature for both the Mojave (~1°C) and the Sonoran (~2°C) portion of the DRECP since 1975. Cayan and colleagues are currently evaluating which of the various climate model results from the more recent IPCC AR5 best fit the California context (pers. comm.).

Desert plants and animals are generally adapted to extreme warm temperatures, but some species may be at or approaching their physiological threshold. While some species may not experience increases in temperature-driven mortality, their survival may nonetheless be affected. For example, the sex determination of eggs laid by desert tortoise is affected by incubation temperature. An incubation temperature of 26°C produces 100 percent male hatchlings while an extra 6 degrees (32°C) produces 100%

female hatchlings (Burke et al. 1996). Furthermore, hatchling vigor can also be impacted by higher temperatures (Spotila et al. 1994). Consequently, it is difficult to predict what effect projected increases in temperature may have on future generations of tortoise.

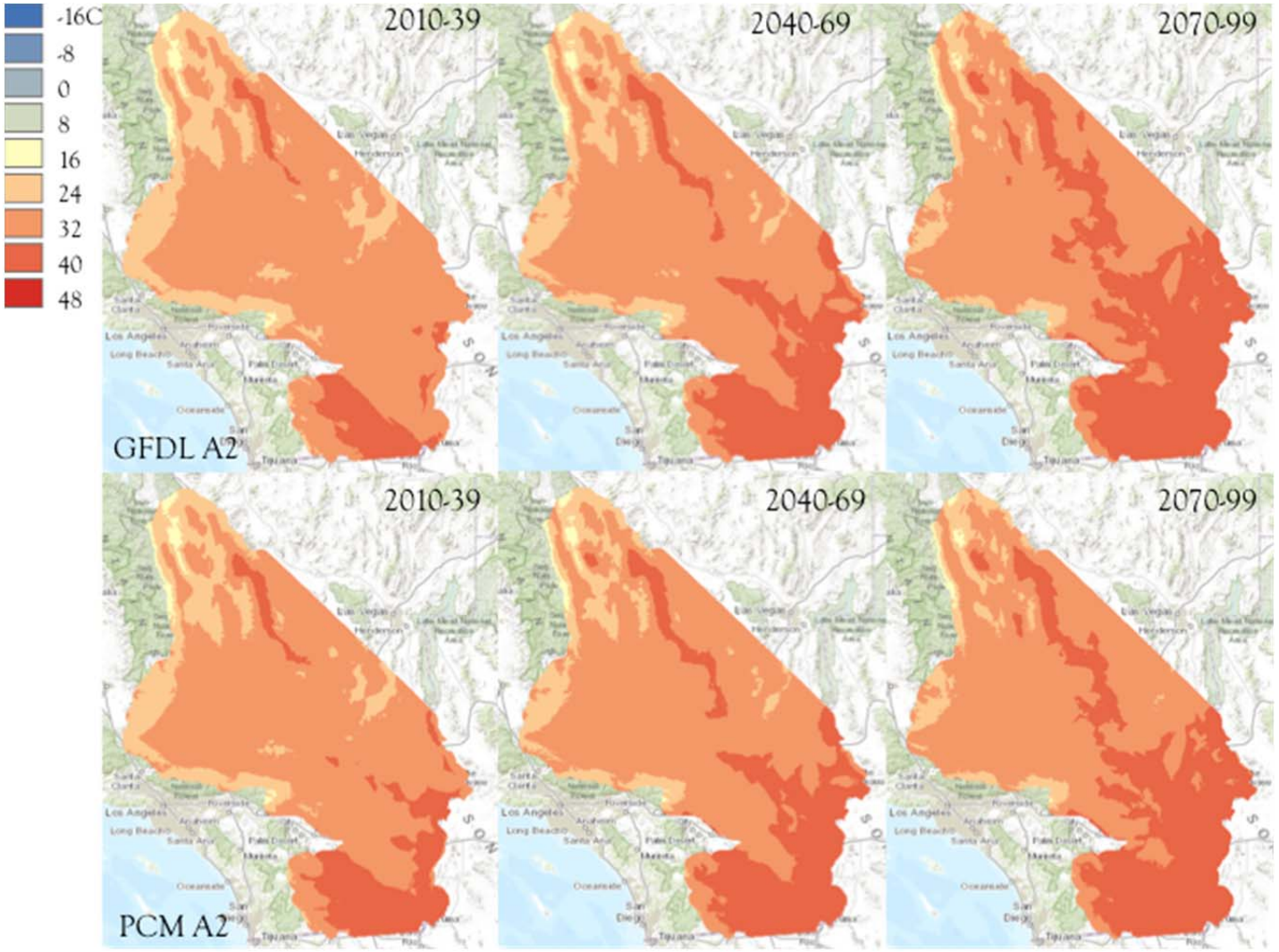

Figure 8. Projected mean annual maximum temperature (in °C) for the DRECP region based on climate data from two GCMs (PCM and GFDL) under the A2 emission scenario at 270m resolution (Flint and Flint, 2012).

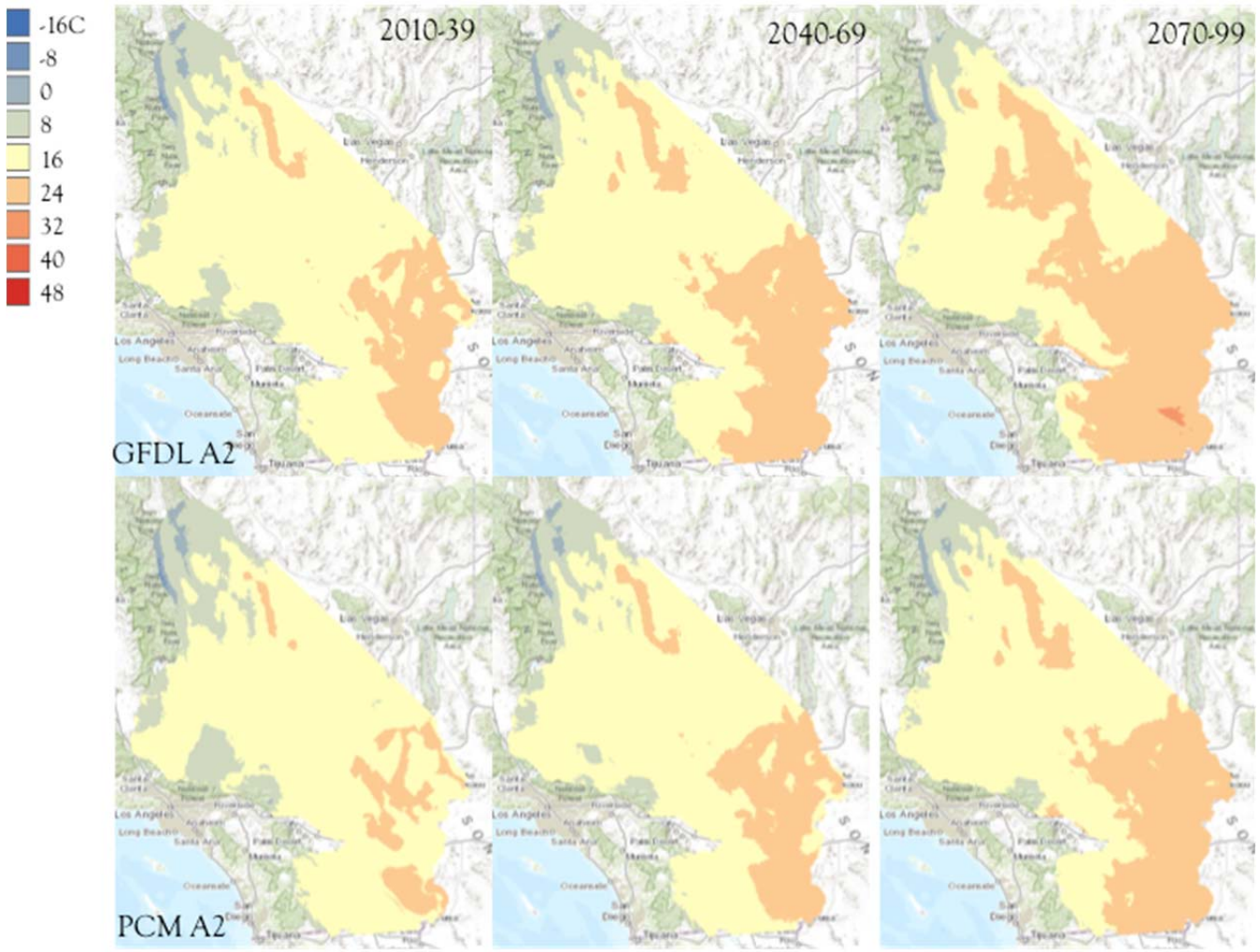

Figure 9. Projected mean annual minimum temperature (in °C) for the DRECP region based on climate data from two GCMs (PCM and GFDL) under the A2 emission scenario at 270m resolution (Flint and Flint, 2012).

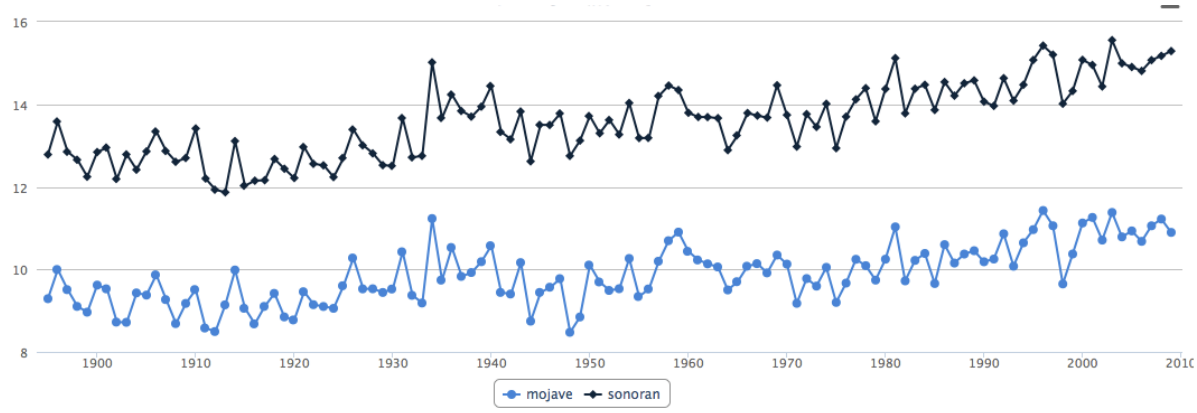

Figure 10. Observed minimum temperature (°C) for the Mojave (blue line) and the Sonoran (black line) from the PRISM climate group (Daly et al. 2008).

Precipitation - AR4

Precipitation in North American deserts is low and varies temporally at both short (season) and longer (decade) time scales (Stahlschmidt et al. 2011). The large variance in precipitation is characteristic of desert areas. A review of recent publications focused on California was provided in a recent PRBO report (2011) that illustrates the range of projections for both the Mojave and Sonoran Deserts for the 21st century (Table 5). Results vary: some GCMs are projecting increases, some decreases in annual rainfall. But given the degree of aridity in the region, even relatively modest changes are likely to have large ecological consequences.

Both GFDL and PCM, the two climate models chosen by Cayan et al. (2008) to evaluate climate change impacts in California, simulate a summer monsoon, but the warmer GFDL scenario projects an overall increase in precipitation while PCM projects a decrease. They both simulate spatial variations in the proportion of summer rainfall over time, but sometimes disagree in the direction of future changes (Figure 11). For example, the fraction of summer rainfall under the A2 emission scenario decreases in the NE corner of the DRECP under the PCM scenario while it increases under GFDL.

Table 5. Summary of published projections of precipitation change in the southern California deserts from various sources (as cited by PRBO 2011 now called Point Blue Conservation Science).

Climate Variable	Mojave	Sonoran	Reference	GCM/RCMs
Mean annual rainfall	-7mm (-5%) to -65mm (42%) ([2038-70 avg] - [1970-99 avg])	+3mm (3%) to -55mm (-45%) ([2038-70 avg] - [1970-99 avg])	Stralberg et al. 2009 cited in PRBO 2011	RegCM3-CCSM3.0 & GFDL CM2.1 A2
	-14mm (NS) [2xCO_2]	-4mm (NS) [2xCO_2]	Bell et al. 2004	RegCM2.5-CCM3
	+12mm (7.7%) [2xCO_2] (1980-99 vs 2080-99)	+8mm (6.2%) 2xCO_2] (1980-99 vs 2080-99)	Snyder and Sloan 2005	RegCM2.5-CSM1.2
Median annual rainfall	-10.3% (NS) [2xCO_2]	-11.8% (NS) [2xCO_2]	Snyder et al. 2004	RegCM2.5-CCM3
Mean rainfall per day	0.2mm (NS) [2xCO_2]	0.00 (NS)	Bell et al. 2004	RegCM2.5-CCM3
Rain days per year	0.9 (NS) [2xCO_2]	-3.2 (NS) [2xCO_2]	Bell et al. 2004	RegCM2.5-CCM3
Extreme rain events	-2.6 days [2xCO_2]	-3.2 (NS)	Bell et al. 2004	RegCM2.5-CCM3

Snowpack

Considering again the two CMIP3 climate model projections (PCM and GFDL under the A2 emission scenario) that had been recommended by Cayan et al. (2008), winter snowpack is projected to decrease under both futures (Figure 12). Until 2040, the "wetter" GFDL maintains a more extensive snowpack than PCM, but that trend does not extend to the 2nd half of the 21st century. Note that under PCM, a slightly higher snowpack is maintained at high elevations in the southern Sierras throughout the 21st century.

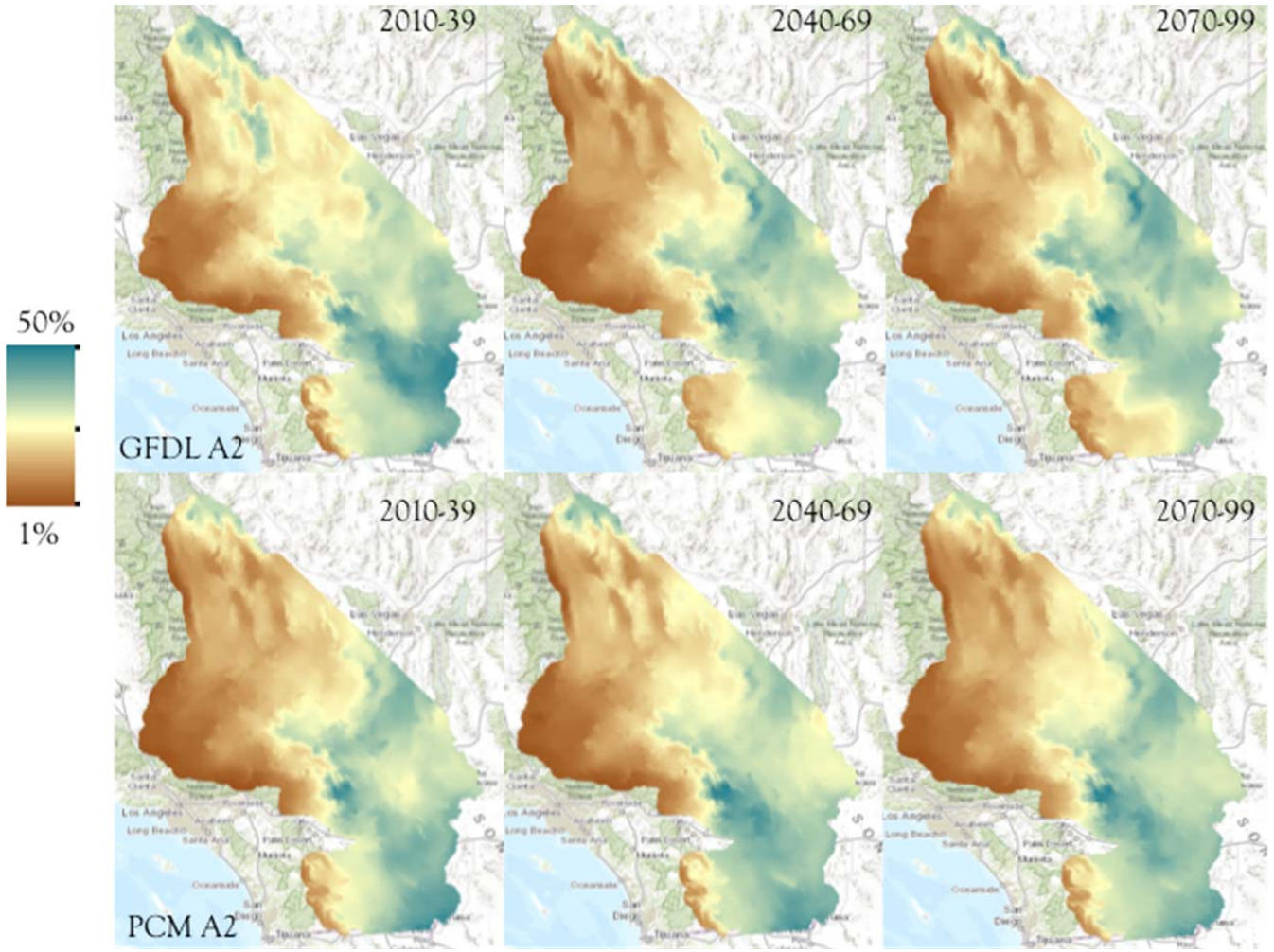

Figure 11. Proportion of summer rainfall simulated by PCM and GFDL climate models under the A2 emission scenario downscaled by Flint and Flint (2012).

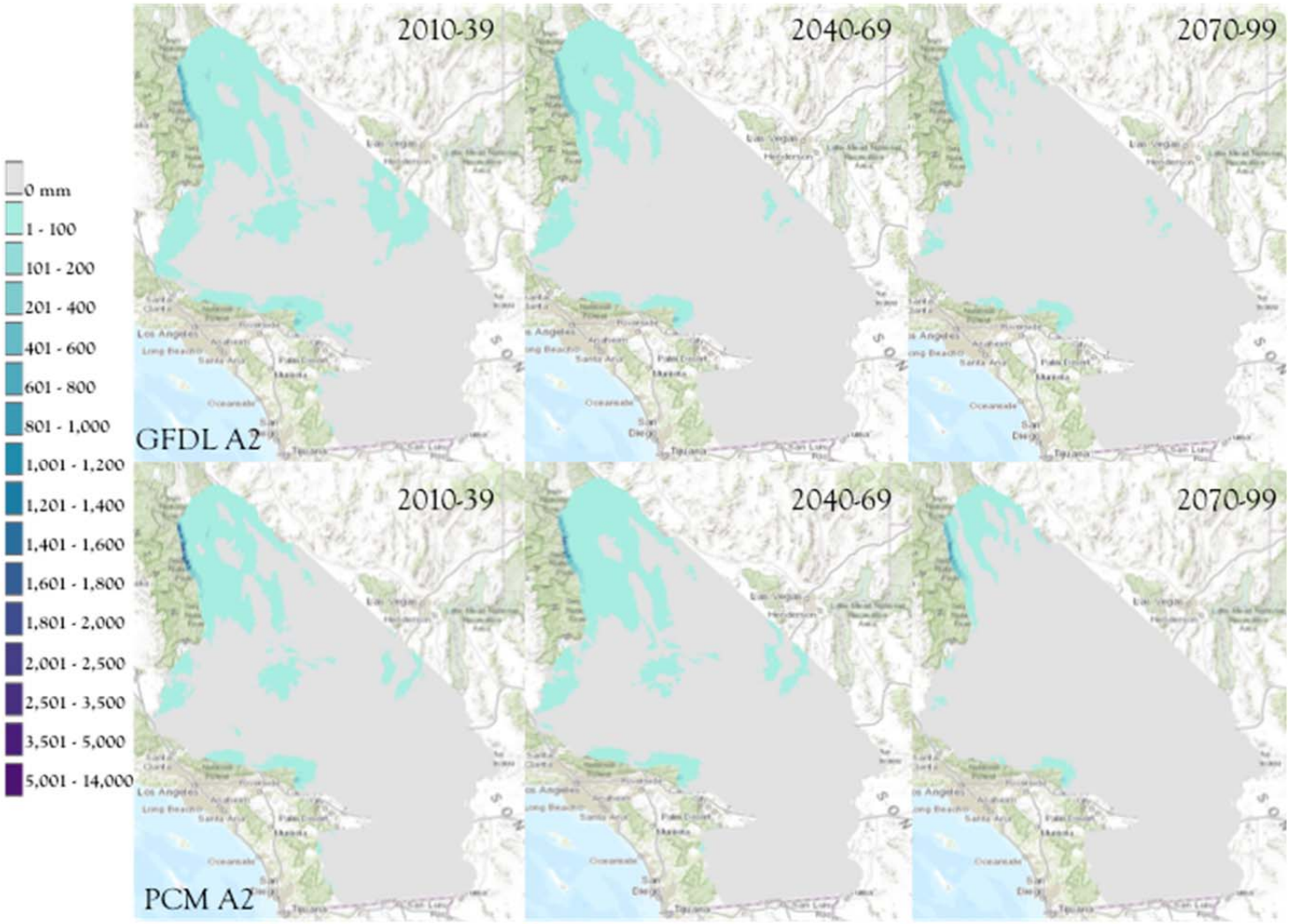

Figure 12. Winter snowpack simulated by PCM and GFDL climate models under the A2 emission scenarios downscaled by Flint and Flint (2012).

Temperature and Precipitation - CMIP5

Focusing on the DRECP region, we examined the most recent downscaled CMIP5 climate model projections (Abatzoglou, 2012). A brief comparison between the earlier CMIP3 futures with these latest results showed good overall consistency between the two sets of climate projections especially with regard to warming trends; all of the models agree on similar levels of warming.

All of the 20 CMIP5 models examined, which were included as part of the latest IPCC AR5, show increases in minimum temperatures compared to historic conditions. Increases in minimum temperature are particularly pronounced with up to 2.7°C under RCP 4.5 scenario and up to 3.5°C under RCP 8.5 scenario (Figure 13). Precipitation projections from these same 20 models show large differences in the magnitude of projected precipitation particularly during summer and winter months (Figure 14). For more detailed climate change analyses conducted for the DRECP region, we only used RCP 8.5 scenario since it appears to be the most likely future; matching closely recent atmospheric CO_2 concentration trend (Figure 15).

There is considerable uncertainty in precipitation projections in general and particularly for California, because California lies between the high latitudes where models agree there will very likely be increases in precipitation and the subtropics where models agree there will be decreases (Neelin et al. 2013). Maloney et al. (2014) reported that, compared to CMIP3 models, CMIP5 projections show a southward shift of the transition zone between the increasing and decreasing winter precipitation that is visible along the West coast of North America. This shift projects more moisture to some parts of California according to many, but not all, climate models.

We chose three CMIP5 climate projections that bracket the range of future precipitation for a similar level of warming over the DRECP region (Figure 16). The three models (MIROC5, CCSM4, and CanESM2) were ranked among the top 10 CMIP5 performers by Rupp et al. (2013) with respect to their ability to simulate historical climate for the west coast of the US and for their overall structural soundness. Each model projects a different precipitation future – one with approximately the same level of winter and summer precipitation as historical but somewhat drier overall (MIROC5), one with wetter winters than historical with similar annual moisture to historical (CCSM4), and one with both much wetter winters and summers than historical (CanESM2). We did not choose a model that simulated drier winters and wetter summers, because there was no model that projected such a future outcome. Because climate model projections include considerable uncertainty, exploring a range of possible futures is realistic. Our approach should help

frame the breadth of potential future regional conditions and allow managers to imagine a range of biological responses to change. As climate conditions continue to be monitored, a close fit between a particular projection and observations might emerge at which time alternative futures will become less meaningful. But until then, considering a range of futures should help managers prepare for potential surprises.

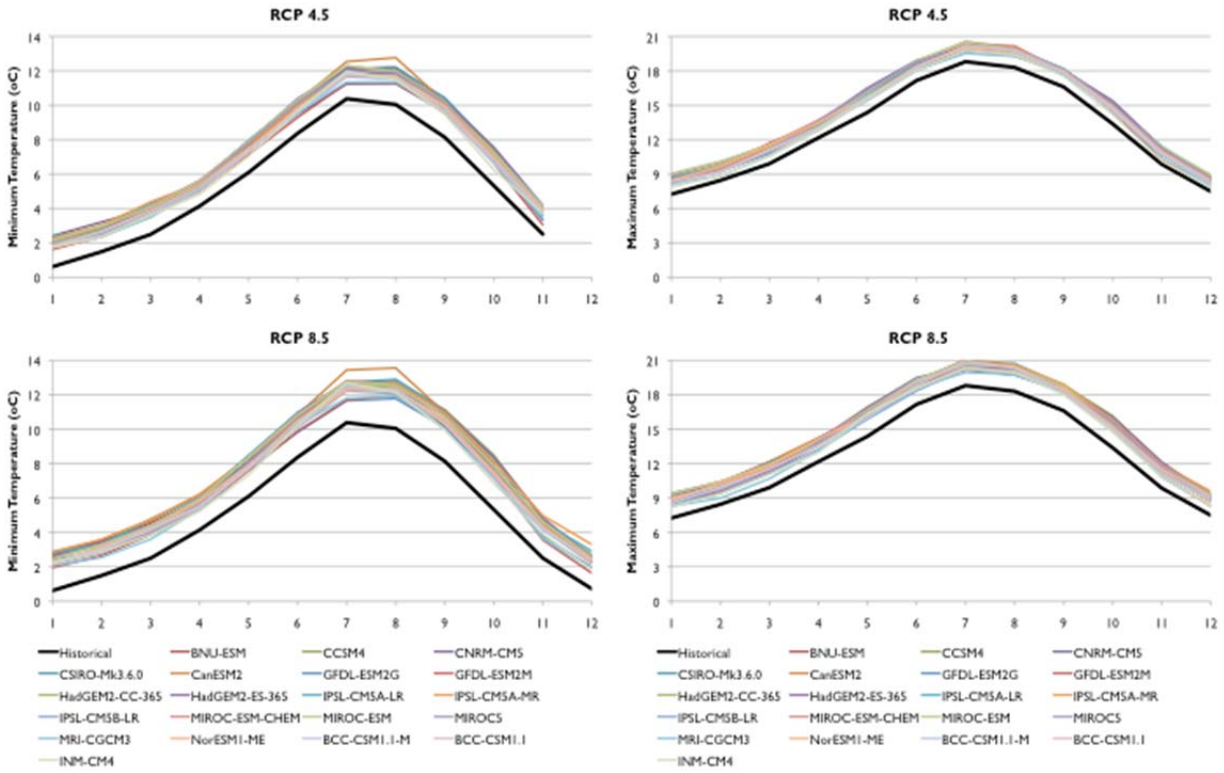

Figure 13. Observed (1971-2000) and projected (2011-2100) minimum and maximum monthly temperature by 20 CMIP5 climate models for two RCP 4.5 (top) and 8.5 (bottom) emission scenarios in the (buffered) DRECP region. Climate data from the various climate modeling teams were downloaded from the CMIP5 site and downscaled by Abatzoglou (2012).

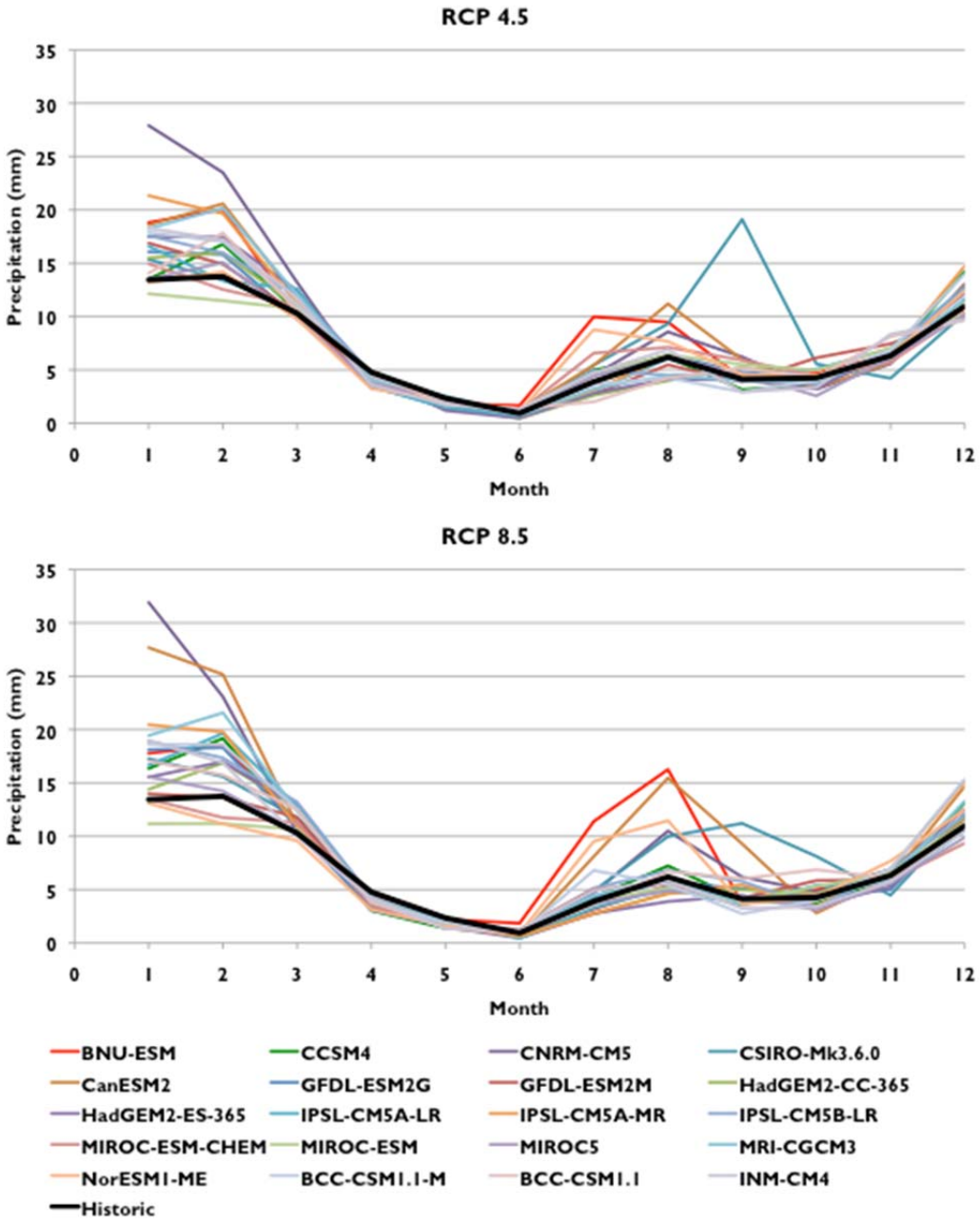

Figure 14. Observed (1895-2010) and projected (2011-2100) monthly precipitation (mm) by 20 CMIP5 climate models for two RCP 4.5 (top) and 8.5 (bottom) emission scenarios in the (buffered) DRECP region. Climate data from the various climate modeling teams were downloaded from the CMIP5 site and downscaled by Abatzoglou (2012).

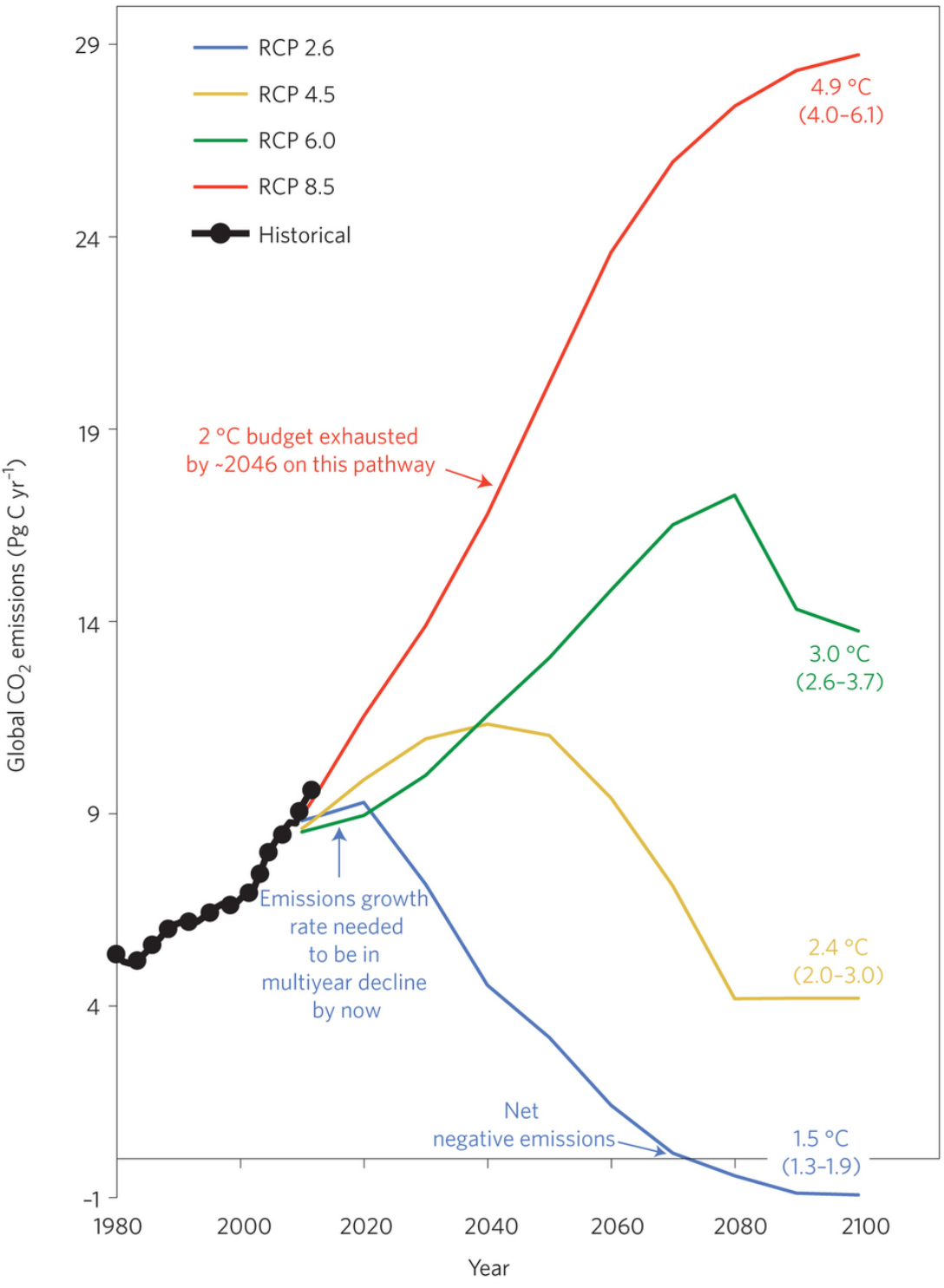

Figure 15. Projection of the atmospheric CO_2 concentration during the 21st century under the AR5 RCP emission scenarios compared to observations (Sanford et al. 2014).

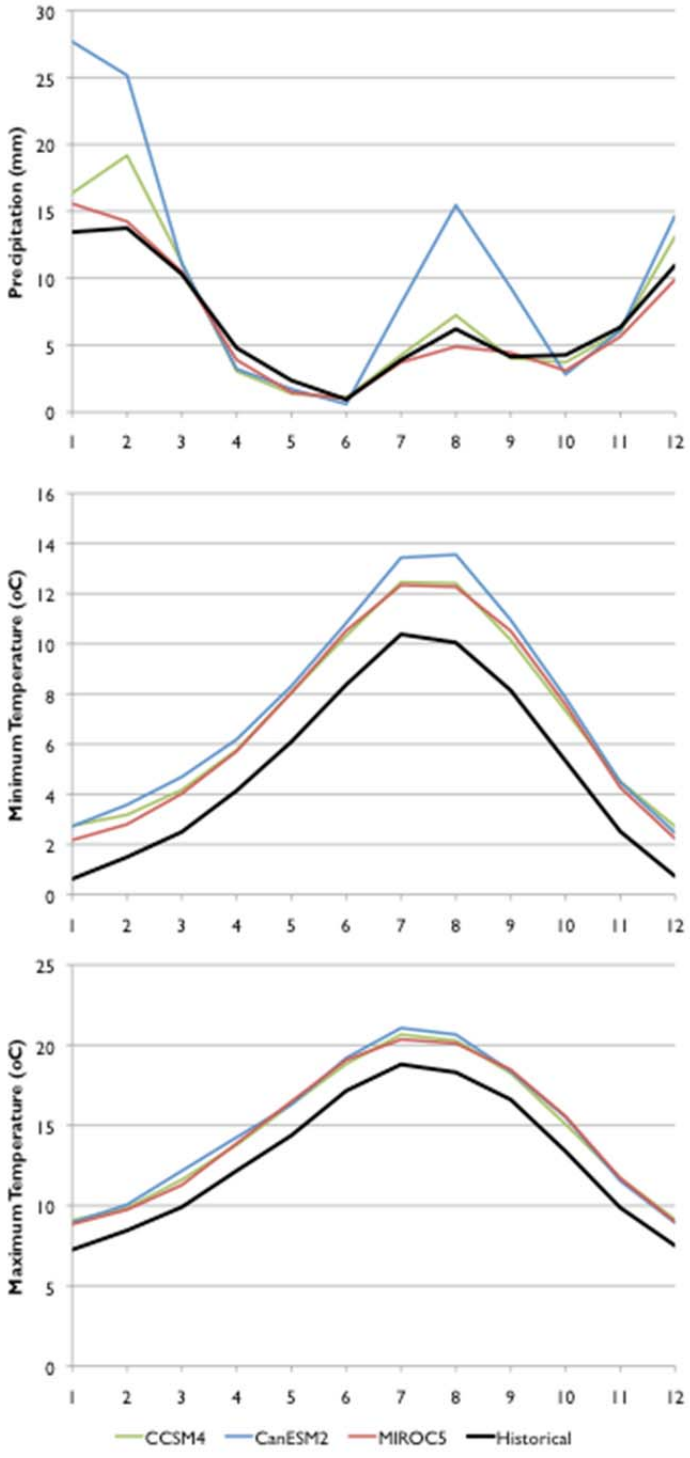

Figure 16. Observed (1895-2011) and projected (2011-2100) monthly average precipitation, maximum and minimum temperature in the (buffered) DRECP region from three CMIP5 climate models (CanESM2, CCSM4, and MIROC5) under RCP 8.5 downscaled by Abatzoglou (2012).

Under the RCP 8.5 emission scenario, the three CMIP5 models (CanESM2, CCSM4, and MIROC5) projected similar gradual increases in annual and seasonal temperature over the next century (2011-2100) with respect to historical conditions (1890-2011) (Figure 17 for the Mojave and Figure 18 for the Sonoran).

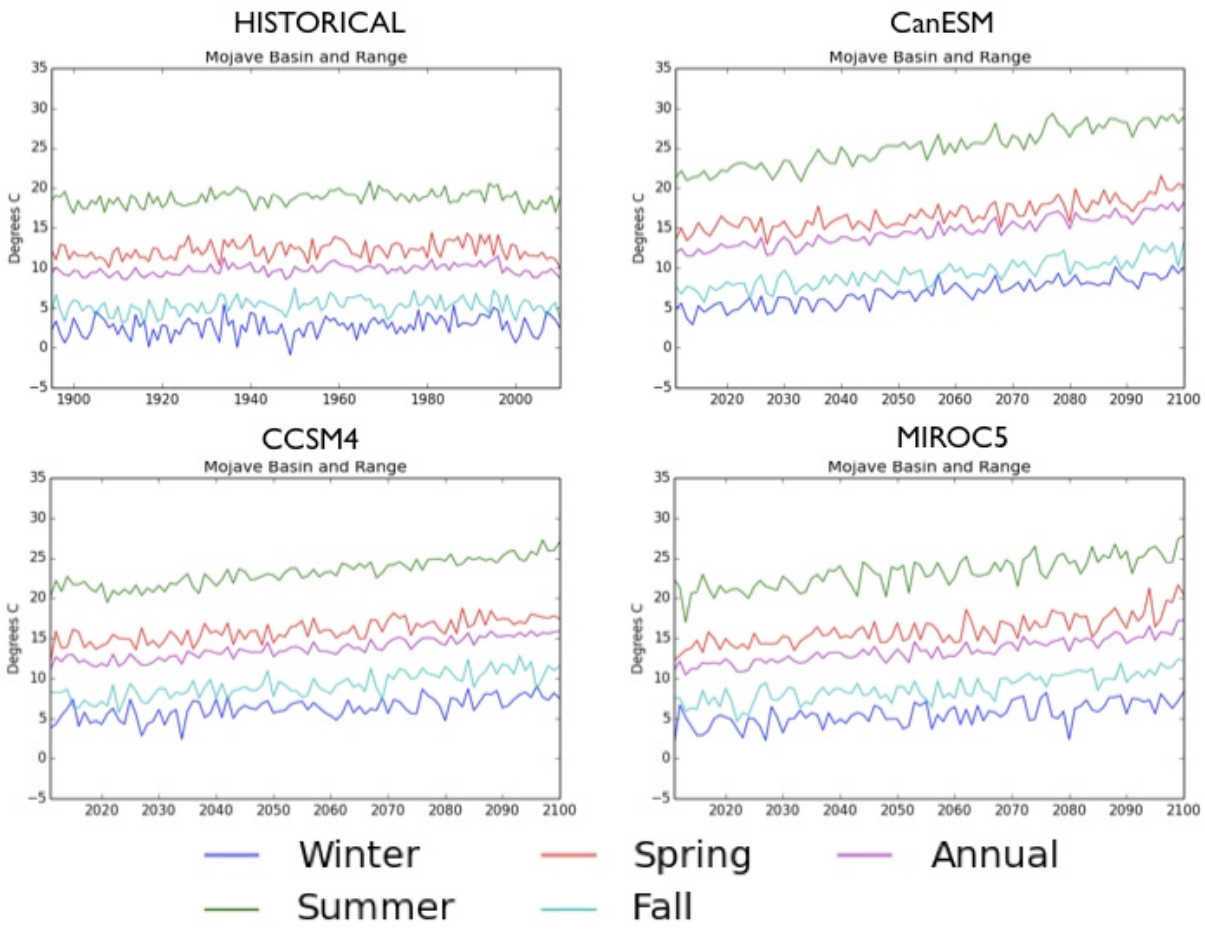

Figure 17. Seasonal and annual minimum temperature (Tmin) for the Mojave portion of the DRECP for the historical (1895-2011) period based on PRISM data (top left) and for the 21st century (2011-2100) projected by three CMIP5 climate models (CanESM2, CCSM4, and MIROC5) downscaled by Abatzoglou (2012).

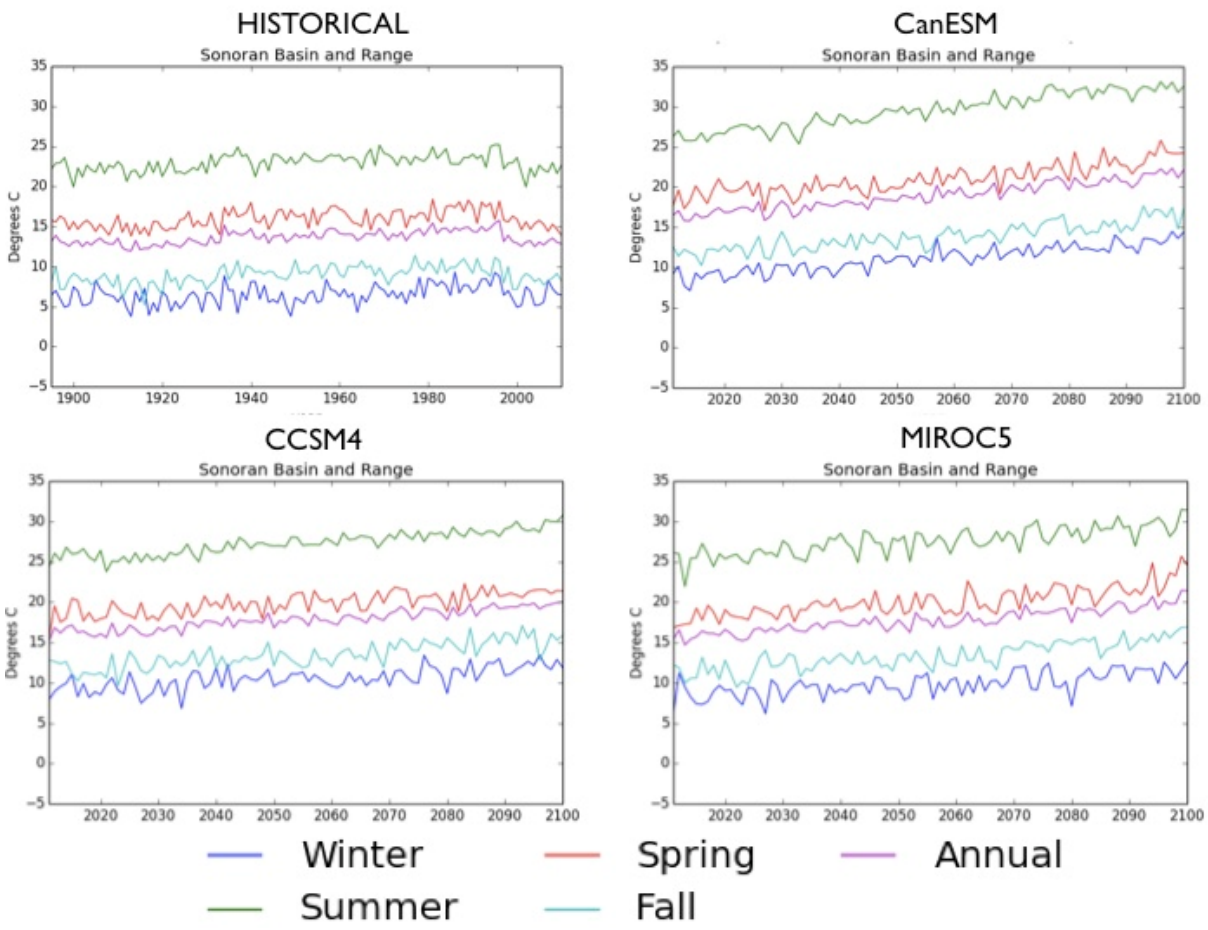

Figure 18. Seasonal and annual minimum temperature (Tmin) for the Sonoran portion of the DRECP for the historical (1895-2011) period based on PRISM data (top left) and for the 21st century (2011-2100) projected by three CMIP5 climate models (CanESM2, CCSM4, and MIROC5) downscaled by Abatzoglou (2012).

For the Mojave Desert portion of the DRECP region, the CanESM2 model projected increasing precipitation throughout the 21st century (Figure 19) with a much wetter future overall despite a decline in spring and to a lesser extent fall rain (Figure 16). Both CCSM4 and MIROC5 models show little trend and very similar year-to-year variability to historical conditions, with higher winter precipitation under CCSM4.

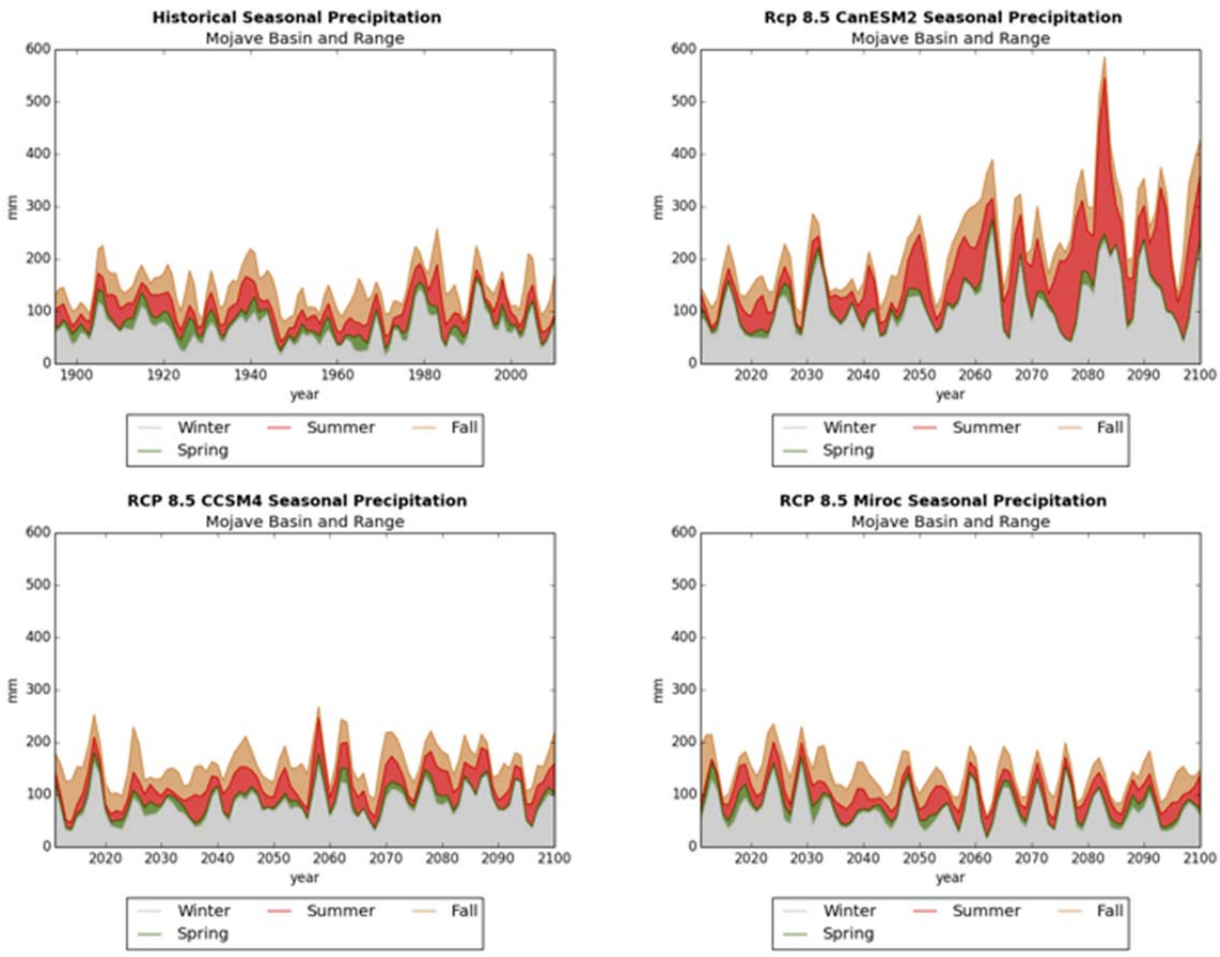

Figure 19. Seasonal and annual precipitation for the Mojave portion of the DRECP for the historical (1890-2011) period based on PRISM data (top left) and for the 21st century (2011-2100) projected by three CMIP5 models (CanESM2, CCSM4, and MIROC5) and downscaled by Abatzoglou (2012).

Results for the Sonoran portion of the landscape, which is generally drier than the Mojave, show comparable precipitation trends (Figure 20). The CanESM2 model is much wetter overall and for all seasons. MIROC5 projections projects lower annual precipitation with a decrease in both summer and fall precipitation particularly during the 2nd half of the 21st century (Figure 16 and 20). CCSM4 projections show similar magnitude of precipitation compared to historical with a shift toward higher winter contributions (Figure 16 and 20). Geil et al. (2014) reviewed the CMIP5 projections to evaluate their skill at simulating the North American monsoon system, which affects the fraction of precipitation received during summer primarily in the Sonoran. Results showed no improvement since CMIP3 in the magnitude of the mean annual cycle of precipitation but significant improvements in

terms of simulating the timing of the seasonal cycle. Geil et al. (2014) conclude that even the highest resolution models are still too coarse to capture small-scale topographically influenced processes that are key to realistically represent the monsoon.

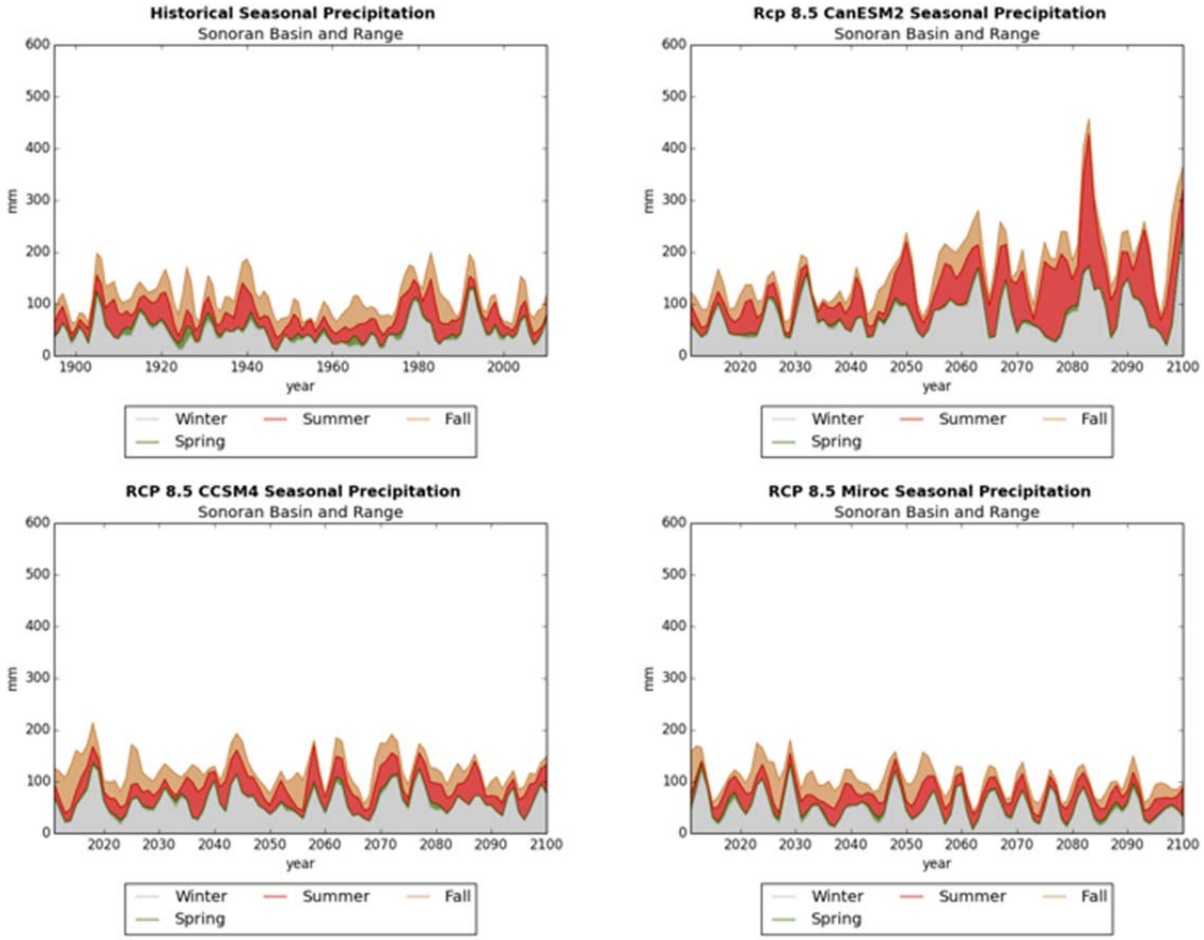

Figure 20. Seasonal and annual precipitation for the Sonoran portion of the DRECP for the historical (1890-2011) period based on PRISM data (top left) and for the 21st century (2011-2100) as simulated by three CMIP5 models (CanESM2, CCSM4, and MIROC5) and downscaled by Abatzoglou (2012).

Hydrological Impacts

The Colorado River flows along the eastern edge of the DRECP region. Projections using CMIP3 climate futures for Colorado River flows showed modest decreases (Christensen and Lettenmaier 2007) and the authors concluded that increased evaporation from warmer temperatures had a greater effect on streamflow than precipitation changes. Similarly, Ficklin et al. (2013) found that in the upper Colorado River Basin, where modest warming are associated with modest precipitation changes in either direction under future climate scenarios, continued rising temperatures are likely to cause drier futures. Harding et al. (2012) used a large number of potential climate futures to simulate streamflow and found decreases 66% of the time, with little change or slight increases in the other 33%. They noted that complex terrain was a complicating factor in the understanding of hydrologic responses to climate change and that relying on few scenarios could bias the results. Despite current efforts to reduce the extensive water diversions for today's agriculture, municipal, and energy development use in southern California, even relatively modest changes in future streamflow are likely to affect the ability of the region to support projected future water use if population density continues to increase and food production intensifies. Consequently, scenarios of reductions in water availability for human use should be considered as the most likely future.

The future streamflow of both the Mojave River, originating in the San Bernardino Mountains, and the Armargosa River, flowing (mostly underground) from its source in a high desert region northwest of Las Vegas, will be affected by projected changes in precipitation and snowmelt patterns. The Mojave River drains the northern slopes of the San Bernardino Mountains and has very little surface flow much of the year along most of its range. It is a classic desert river with a large groundwater supply that supports development and irrigated agriculture in the valley. The Amargosa River is important in this arid part of the desert because it supports vital habitat for a variety of birds and aquatic organisms. A 12-mile section has been nominated as a Wild and Scenic River designation.

Flint and Flint (2012) did a thorough investigation of the most important aspects of the hydrological impacts of climate change in California using the recommended PCM and GFDL climate projections. For the DRECP region, the message was clear: overall drier conditions (Figure 21) with less soil moisture and less recharge, but spatial variations are to be expected and permanent streams with riparian corridors will likely become refuge islands for species at risk from extreme heat and evaporative demand.

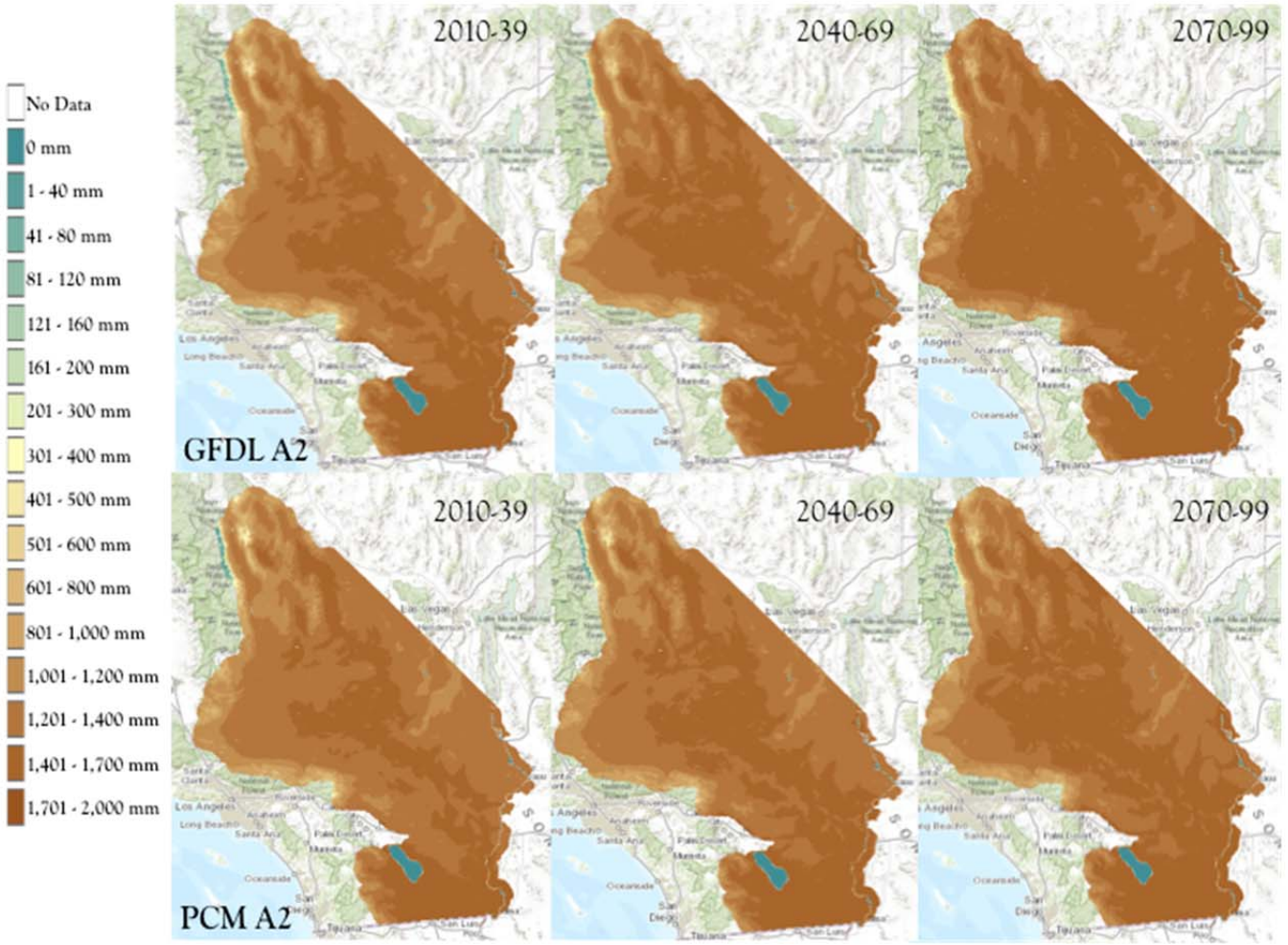

Figure 21. Climate Water Deficit (PET-AET) simulated by the Basin Characterization Model (BCM) using the PCM and GFDL A2 climate futures for three time periods (Flint and Flint 2012)

Vegetation and Fuels Modeling

Brief Overview of the Method Used

Using inputs from three CMIP5 models, we simulated potential vegetation response using the Dynamic Global Vegetation Model (DGVM) MC2. MC2 is the C++ version of MC1 (e.g. Bachelet et al. 2008) that simulates vegetation distribution, biogeochemical cycling, and wildfire in a highly interactive manner. The model does not simulate plant species, but rather broad vegetation types composed of lifeforms defined as woody or herbaceous with various leaf morphologies (needleleaf or broadleaf) and phenologies (deciduous or evergreen). It simulates the competition between these lifeforms for light, water, and nutrients. The model simulates potential vegetation i.e. the vegetation that would occur on the landscape given local climate and soil conditions while ignoring land use legacies from human occupation. Consequently, vegetation model simulation results for current conditions often disagree with reality. However, projected potential vegetation dynamics under future conditions provide valuable insights on how native vegetation may respond to climate change while projections of future land use are highly uncertain. Moreover, relying on predicted changes in a particular species range (contraction or expansion) alone can bring surprises when an extreme climate event or pest outbreak extirpates such species, or if invasive or "climate refugee" species take over.

The model simulates carbon and nitrogen cycling, allocating material among plant parts, multiple classes of leaf litter, and soil organic matter pools. Production is calculated monthly and is limited by temperature, soil water availability, nitrogen, and atmospheric CO_2 (Bachelet et al. 2001). The model also simulates actual and potential evapotranspiration (AET and PET) as well as soil water content to reflect water use by the vegetation. Live and dead plant material is interpreted as fuel categories and their daily moisture is used to modulate fire occurrence and behavior (Lenihan et al. 2008). Potential fire behavior is modulated by vegetation type, which affects fuel properties and realized wind speeds (higher for herbaceous than woody lifeform-dominated systems).

The MC2 model uses inputs on soil depth, texture, and bulk density as well as monthly precipitation, minimum and maximum temperatures, and vapor pressure. Historical climate data (1895-2010) were created and distributed by the PRISM group at Oregon State University (Daly et al. 2008) and future CMIP5 climate projections (2010-2100) were downscaled using a method developed by Abatzoglou (2011) and provided through his web site (http://maca.northwestknowledge.net/).

Vegetation Model Results

MC2 DGVM results were simplified by combining several vegetation types into four basic ones to facilitate interpretation (Figure 22 for Mojave and Figure 23 for Sonoran portions of the DRECP). Woody plants (dark green) represent trees and shrublands, from dense woodlands to sparse shrublands. Herbaceous plants (yellow) include grasses, sedges, and forbs. Desert (red) defines low to negligible productivity areas and is characterized on the ground by sparse woody and/or herbaceous cover. Barren land (black) defines bare rock and soil that do not support plant growth.

Because of its greater winter rains under historical conditions, larger portions of the Mohave are dominated by woody lifeforms (Figure 22) than in the drier Sonoran (Figure 23). The herbaceous cover is also more prominent in the Mojave because of its generally greater soil surface water availability particularly in winter and spring. The Sonoran is dominated by desert where herbaceous plants can dominate during wetter periods and barren land can emerge during particularly dry periods. Sparse woody vegetation can remain on desert landscapes for extended periods of time, both in times of higher moisture as well as prolonged drought.

Under the wetter future projected by the Canadian earth system model (CanESM2), woody vegetation expands steadily across the Mojave but only slightly in the Sonoran. Desert and barren lifeforms decline in the Mojave by the end of the century as increasing rains cause the Sonoran to become increasingly dominated by herbaceous vegetation.

The warmer, somewhat drier future projected by MIROC5 promotes the persistence of the desert area with an increase in the extent of barren land in the Mojave, particularly after 2050. The Sonoran desert is subject to a early period of herbaceous dominance that is quickly followed by an increasing trend in desert and barren areas.

The vegetation model under the CCSM4 future simulates modest increases in herbaceous cover and a decline in desert area in the Mojave. Decadal variability appears less pronounced than during the historical period. Because of its projected increase in winter rain, the CCSM4 future also causes a large increase in herbaceous cover in the Sonoran at the expense of desert areas.

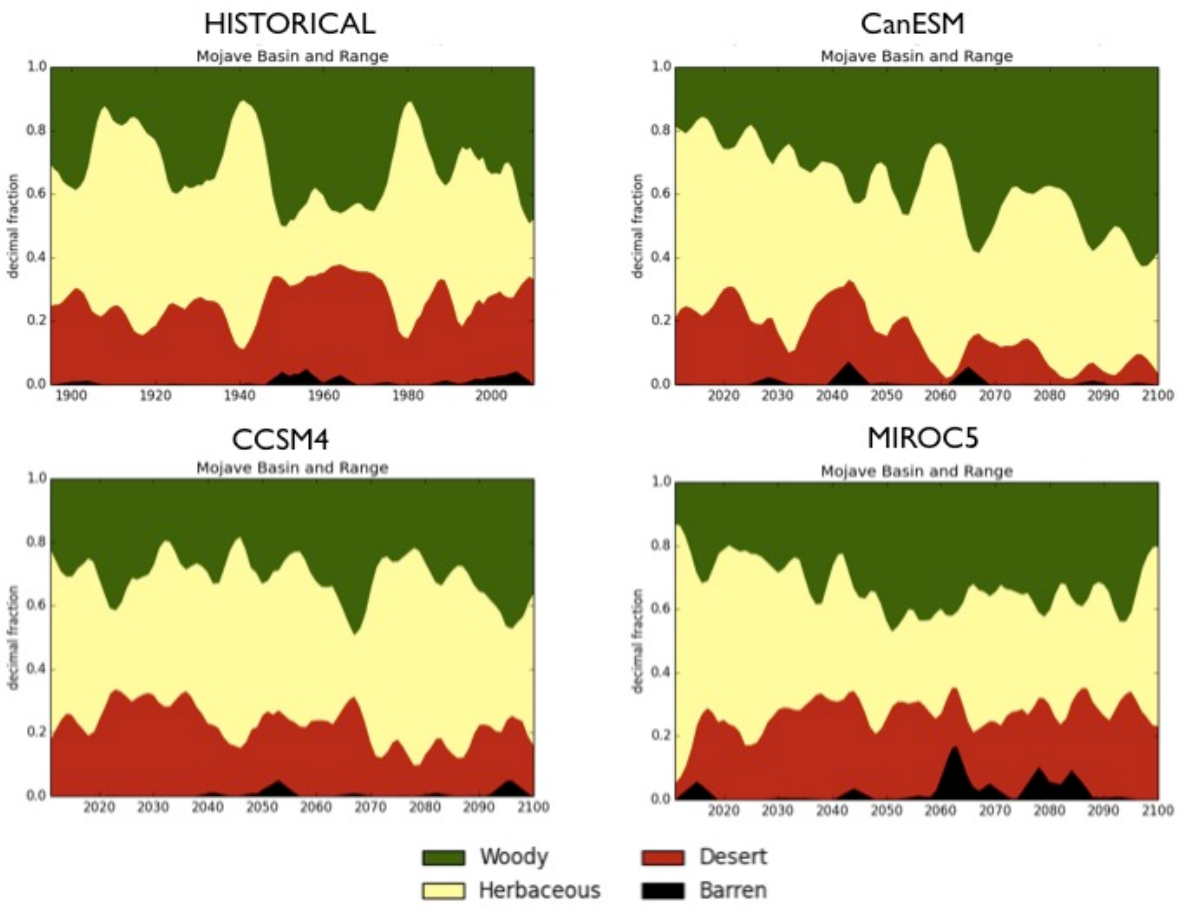

Figure 22. Potential vegetation dynamics over the Mojave region of the DRECP for the historical (1890-2011) and future (2011-2100) periods simulated by the MC2 model using three CMIP5 climate model projections (CanESM2, CCSM4 and MIROC5) under RCP 8.5 downscaled by Abatzoglou (2012). A 15 year smoothing algorithm was used to display the model results.

Each of the CMIP5 futures is characterized by a different spatial distribution of the aggregated potential vegetation types. With CanESM2 climate future, the wettest model of the three presented here, the MC2 model simulated a steady decline in desert areas (already shown in Figure 22) durng the 21st century due to the expansion of the woody vegetation (woodlands and shrublands) driven by increased winter precipitation in the Mojave portion of the region. We simulated increases in herbaceous cover throughout the Sonoran simply caused by the general increase in annual precipitation (Figure 24).

The MIROC5 climate future (the driest of the three) caused significant declines in herbaceous cover in the Mojave as surface water availability declines under warmer conditions (Figure 25). Woody vegetation (xeromorphic shrublands) can expand because

of its ability to access deeper water in the soil profile recharged during the winter season (increased winter rainfall) and because of the simulated CO_2 fertilization effect whereby water use efficiency increases in step with the atmospheric CO_2 concentration. In the Sonoran portion of the DRECP, the desert expands at the expense of the herbaceous dominated systems and barren areas appear.

The CCSM4 climate future, characterized by similar precipitation levels to those observed in the 20th century but with somewhat wetter winters, caused a modest expansion of the woody vegetation by end of the century in the Mojave and large increases in herbaceous cover throughout the entire region, especially in the Sonoran (Figure 26).

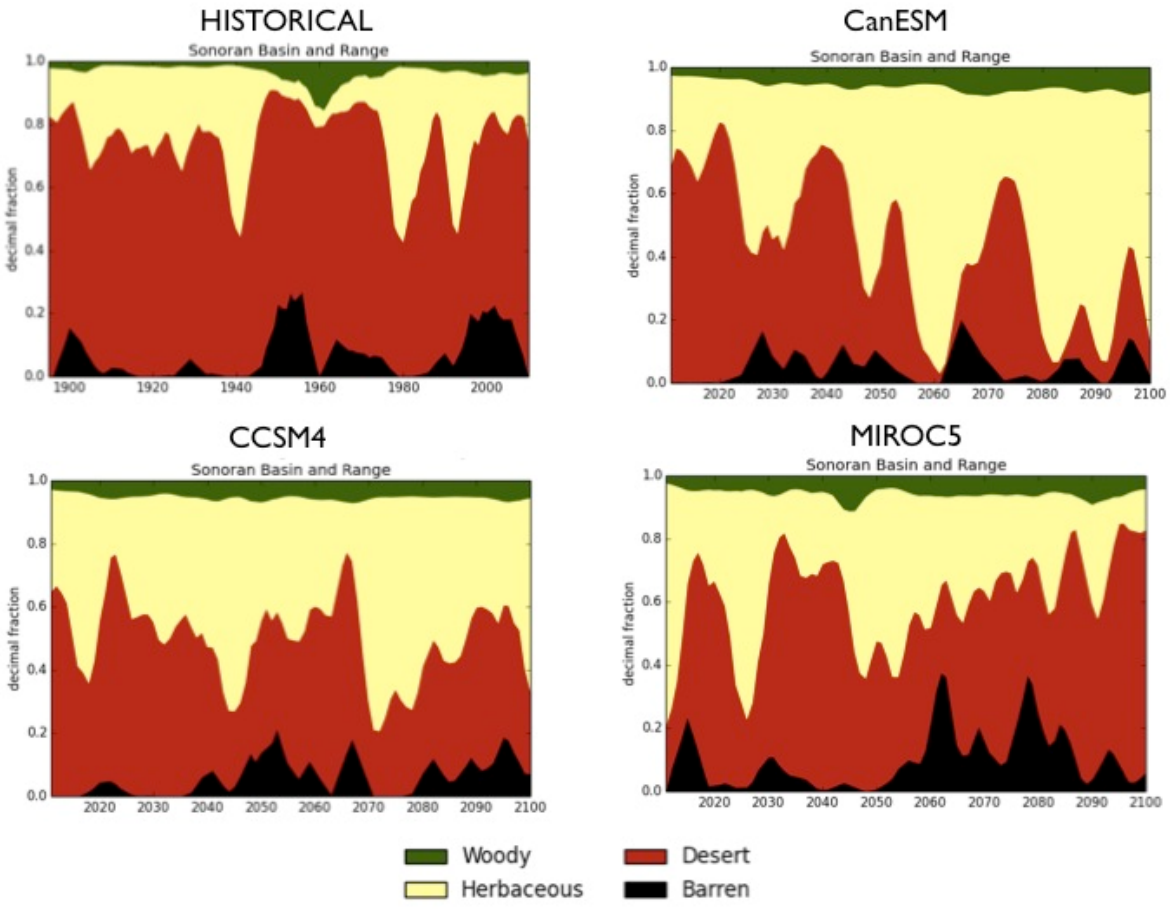

Figure 23. Potential vegetation dynamics over the Sonoran region of the DRECP for the historical (1890-2011) and future (2011-2100) periods simulated by the MC2 model using three CMIP5 climate model projections (CanESM2, CCSM4 and MIROC5) under RCP 8.5 downscaled by Abatzoglou (2012). A 15 year smoothing algorithm was used to display the model results.

Note that the Figures 24, 25, and 26 illustrate the most frequent (mode) potential vegetation type for a given location in map form over each time period while the time series graphs in Figures 22 and 23 show year-to-year variability dominated by each vegetation type across the entire region.

Because barren lands are sparse and simulated only under the driest of conditions (MIROC5) by the vegetation model, we created a "barren index" based on the percent time it was simulated as dominant over a 30-year period. With the wet CanESM2 climate future, there is an overall decline in barren land, but certain areas (e.g., Death Valley) are most likely to remain the more barren portions of the DRECP landscape (Figure 27). As expected, the driest MIROC5 climate future causes an overall increase in the barren index (Figure 28). The CCSM4 climate future causes an early century decline in barren lands due to high precipitation levels in the earlier part of the 21st century (Figures 19 and 20) followed by a renewed mid-century expansion, ending with conditions fairly similar to those found during the historical period (Figure 29).

In the MC2 DGVM, herbaceous lifeforms successfully compete with woody lifeforms for surface water (often ephemeral) while woody lifeforms have access to deeper (phreatophytic) water reserves in the profile. This assumption fits many observations throughout the world. In the DRECP region, the survival of phreatophytic mesquite and the extirpation of the grasslands have been attributed to the shrub capacity to grow deeper roots as the water table dropped such as at Harper's well which agrees well with our model structure. Along the same lines, wet springs, the precipitation pulses described by Moritz et al. (2012) can cause extensive blooms in the desert that are simulated in our model as times of herbaceous expansion, even if ephemeral that year.

In the last 2 decades of the 21st century, higher temperatures and evaporative demand have caused increases in fire frequency throughout the dry forests of the western US (Westerling et al. 2006). In California, further increases in temperature will likely cause more fires in the Sierra Nevada and in chaparral where high human population densities ensures enough fire ignition sources. Desert areas with sparse vegetation, however, do not have a history of fire since fuel loads are so low, and, more importantly, too discontinuous to carry a fire. Moritz et al. (2012) remarked that, in some deserts, fire activity has been increasing because of invasive herbaceous species (D' Antonio and Vitousek 1992, Brooks et al. 2004). Any future increases in annual precipitation could exacerbate this trend, although in desert areas such as the Sonoran, temperature increases will likely outweigh precipitation increases reducing the likelihood of fuel build-up.

Historic (1971-2000) **CanESM2 (2036-2065)** **CanESM2 (2071-2100)**

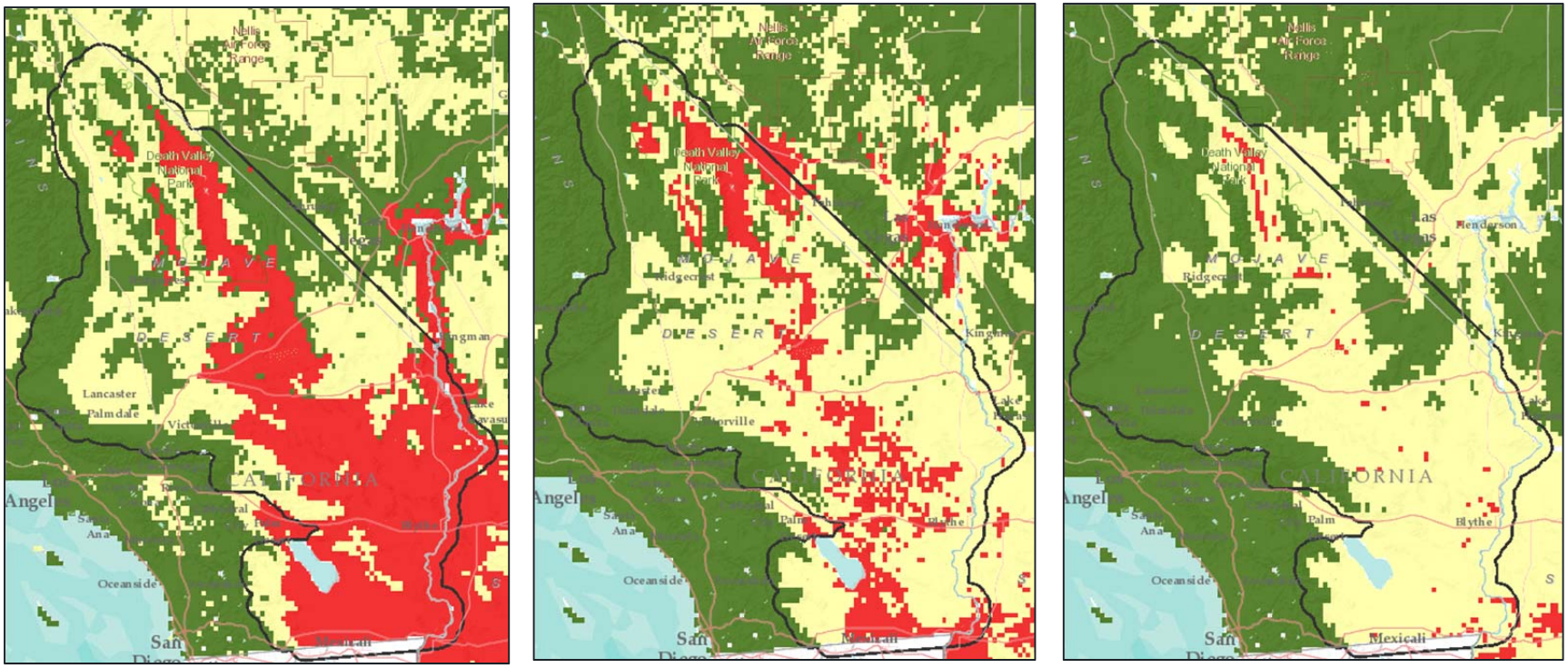

Figure 24. Potential vegetation distribution simulated by the MC2 DGVM over the DRECP region for the historical (1971-2011) period using PRISM climate drivers and for two future periods (2036-2065 or mid-century and 2071-2100 or late-century) using CanESM2 future climate downscaled by Abatzoglou (2012) (green = woody, yellow = herbaceous, red = desert).

Historic (1971-2000) **MIROC5 (2036-2065)** **MIROC5 (2071-2100)**

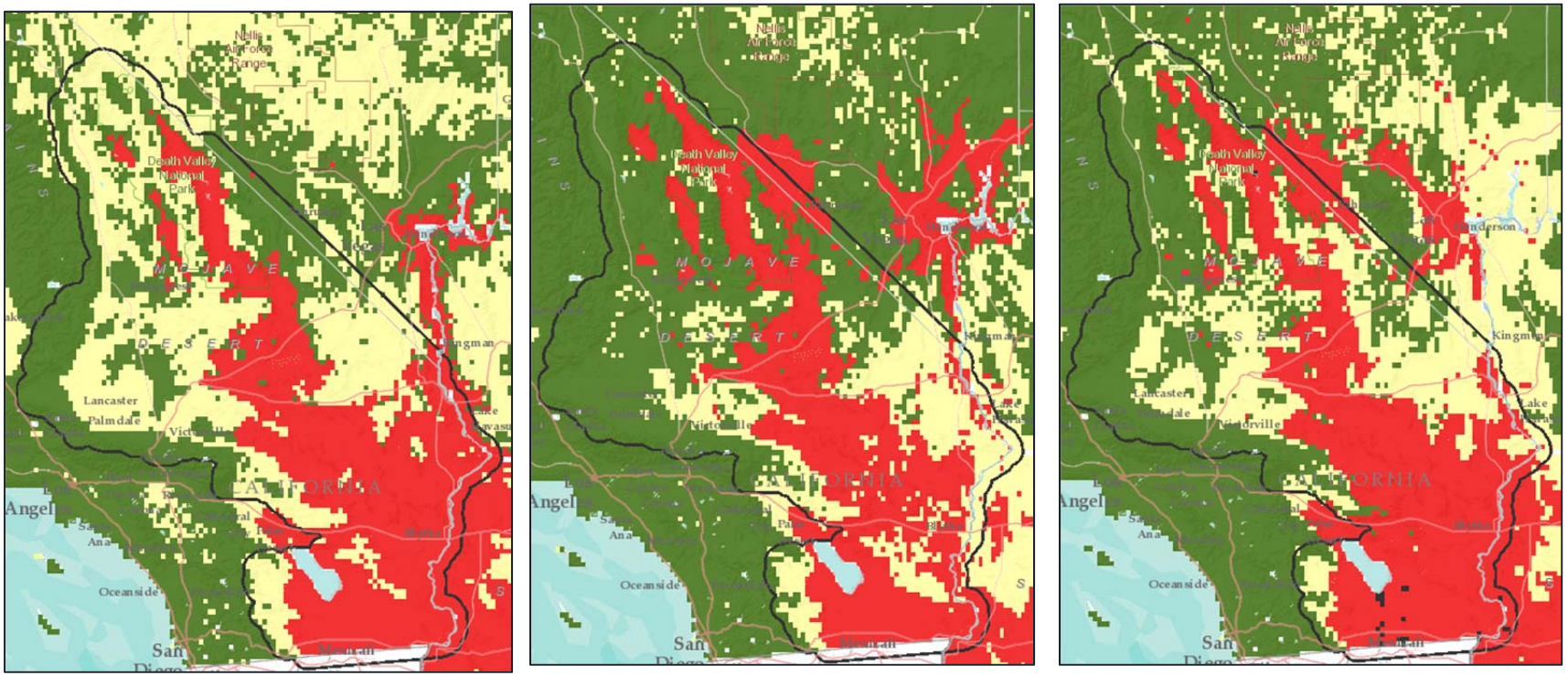

Figure 25. Potential vegetation distribution simulated by the MC2 DGVM over the DRECP region for the historical (1971-2011) period using PRISM climate drivers and for two future periods (2036-2065 or mid-century and 2071-2100 or late-century) using MIROC5 future climate downscaled by Abatzoglou (2012) (green = woody, yellow = herbaceous, red = desert).

Historic (1971-2000) **CCSM4(2036-2065)** **CCSM4 (2071-2100)**

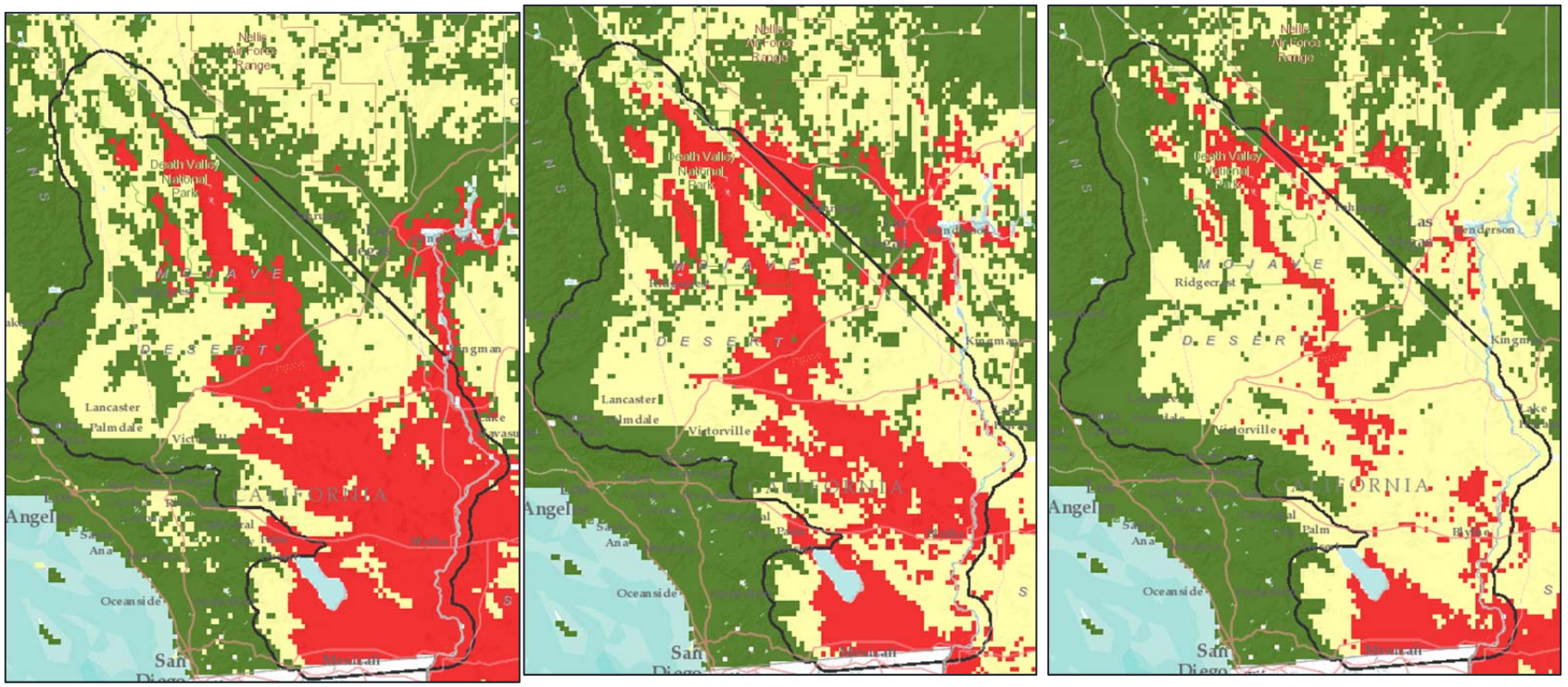

Figure 26. Potential vegetation distribution simulated by the MC2 DGVM over the DRECP region for the historical (1971-2011) period using PRISM climate drivers and for two future periods (2036-2065 or mid-century and 2071-2100 or late-century) using CanESM2 future climate downscaled by Abatzoglou (2012) (green = woody, yellow = herbaceous, red = desert).

Historic (1971-2000)

CanESM2 (2011-2040)

CanESM2 (2041-2070)

CanESM2 (2071-2090)

Figure 27. Barren land index based on MC2 DGVM results driven with CanESM4 climate future under the RCP 8.5 emission scenario and downscaled by Abatzoglou (2012).

Historic (1971-2000)

MIROC5 (2011-2040)

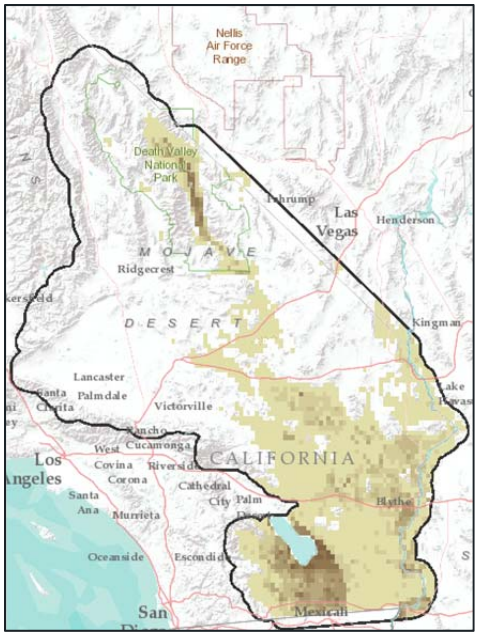

MIROC5 (2041-2070)

MIROC5 (2071-2090)

Figure 28. Barren land index based on MC2 DGVM results driven with MIROC5 climate future under the RCP 8.5 emission scenario and downscaled by Abatzoglou (2012)..

Historic (1971-2000)

CCSM4 (2011-2040)

CCSM4 (2041-2070)

CCSM4 (2071-2090)

Figure 29. Barren land index based on DGVM results driven with CCSM4 climate future under the RCP 8.5 emission scenario and downscaled by Abatzoglou (2012).

Climate Change Refugia

We defined climate change refugia as areas where organisms may be able to survive, at least temporarily, conditions assumed to shift beyond their tolerance limits. We defined two sets of criteria to locate climate refugia. First we identified areas where physical characteristics ("enduring features") should be able to mitigate change to a certain degree (named "physical refugia" from this point forward) and secondly, areas where the projected changes in climate are expected to be the least (named "climate refugia" from this point forward). Using the Environmental Evaluation Modeling System (EEMS), we developed logic models to identify these areas within the DRECP region and produced summary maps of their location (at both 270m and 1km resolution).

To identify the physical refugia, we took into account proximity to water bodies (broken out in four size classes), stream density, ephemeral water density (playas and seeps/springs), topographic shade density, and riparian vegetation density. Each of these factor was converted into a set of fuzzy values. We then defined thresholds for each converted factor in a logic model (Figure 30) to locate the most valuable physical refugia (MVPR). Results show that MVPRs commonly occur in topographically rough areas, for example in canyons and valleys, as well as along the Colorado River (Figure 31). Less valuable but nonetheless important refugia in this desert occur in a few areas where either permanent or ephemeral water bodies occur and around the Salton Sea.

PCM and GFDL climate projections available at the finest, most appropriate, spatial resolution were used to locate climate refugia in the DRECP region. We used changes from historical conditions (1970-1999) in: (1) winter minimum temperature, (2) summer maximum temperature, (3) annual temperature range, (4) winter precipitation, (5) summer precipitation, and (6) total precipitation. The greatest change in each of these variables was converted into a fuzzy value that was used in a logic model (Figure 32) at each grid cell to evaluate its value as a climate refugium. As expected, when we compared changes across three time periods (2010-2039, 2040-2069, and 2070-2099) we found the greatest changes had occurred at the end of the century. Results using GFDL projections showed the greatest level of change across the entire area but under both PCM and GFDL climate futures the central part of the study area showed the most moderate change (Figure 33).

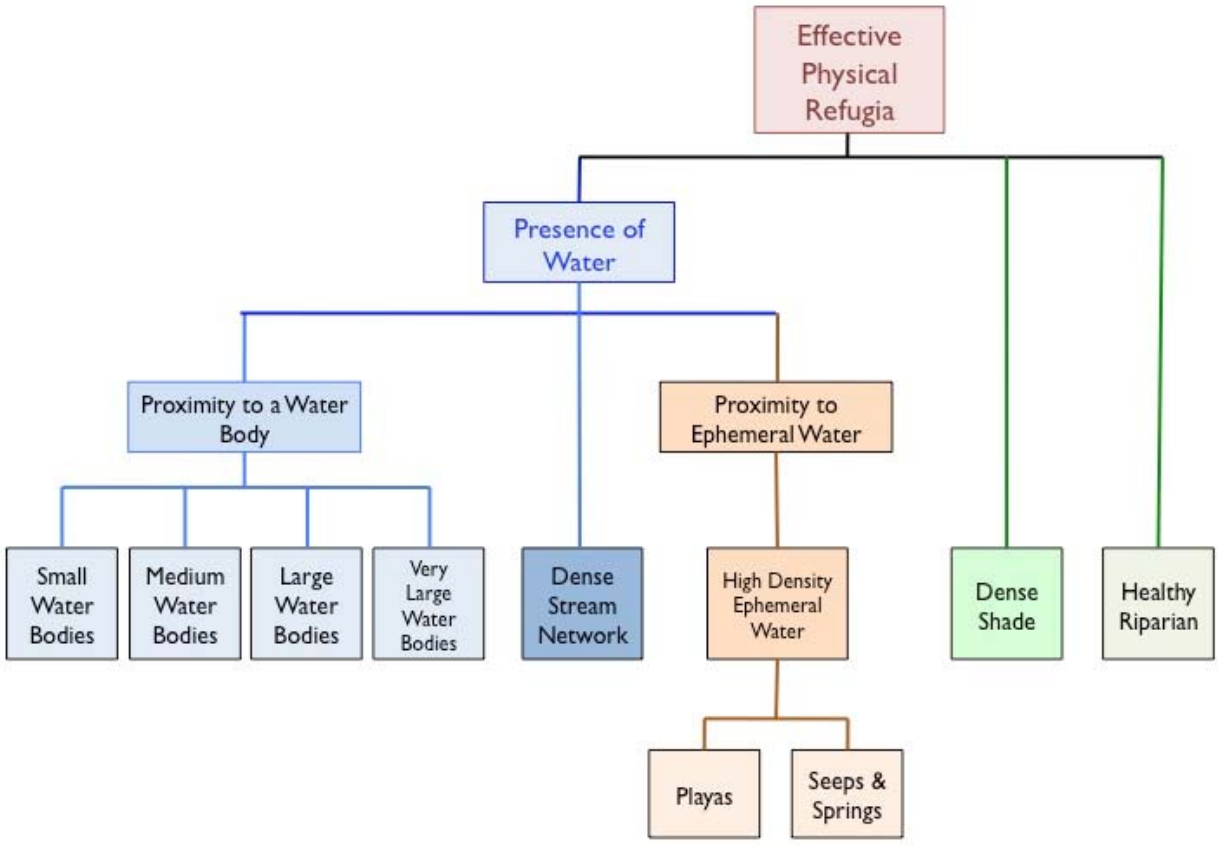

Figure 30. Simplified EEMS fuzzy logic model showing the datasets used to identify the most valuable physical refugia.

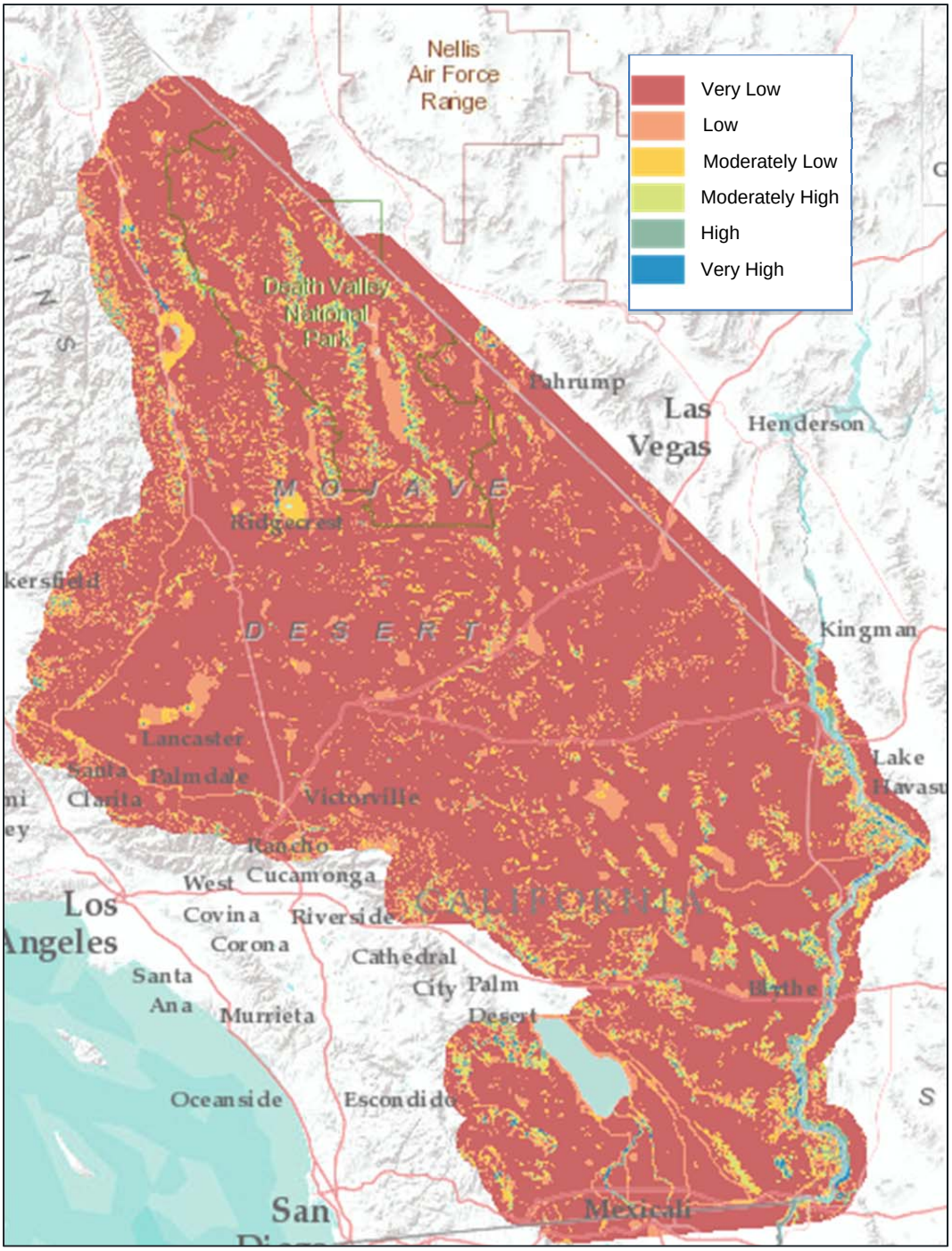

Figure 31. Location of physical refugia of different value within the DRECP study area (1km resolution).

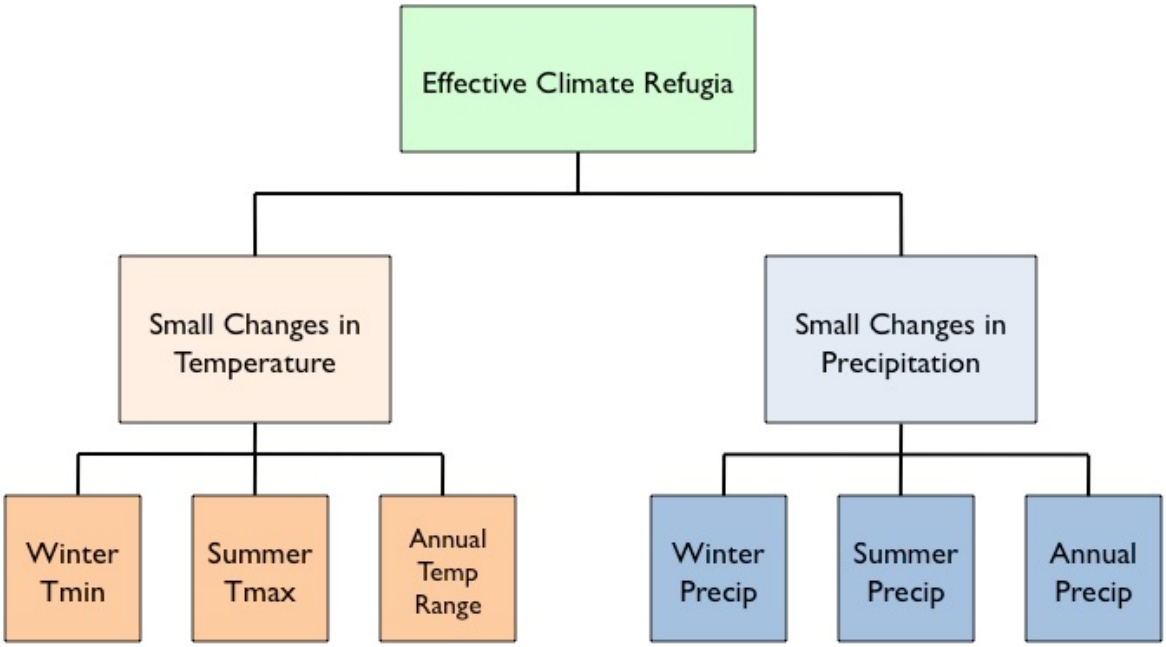

Figure 32. Simplified EEMS fuzzy logic model to identify the most valuable climate refugia.

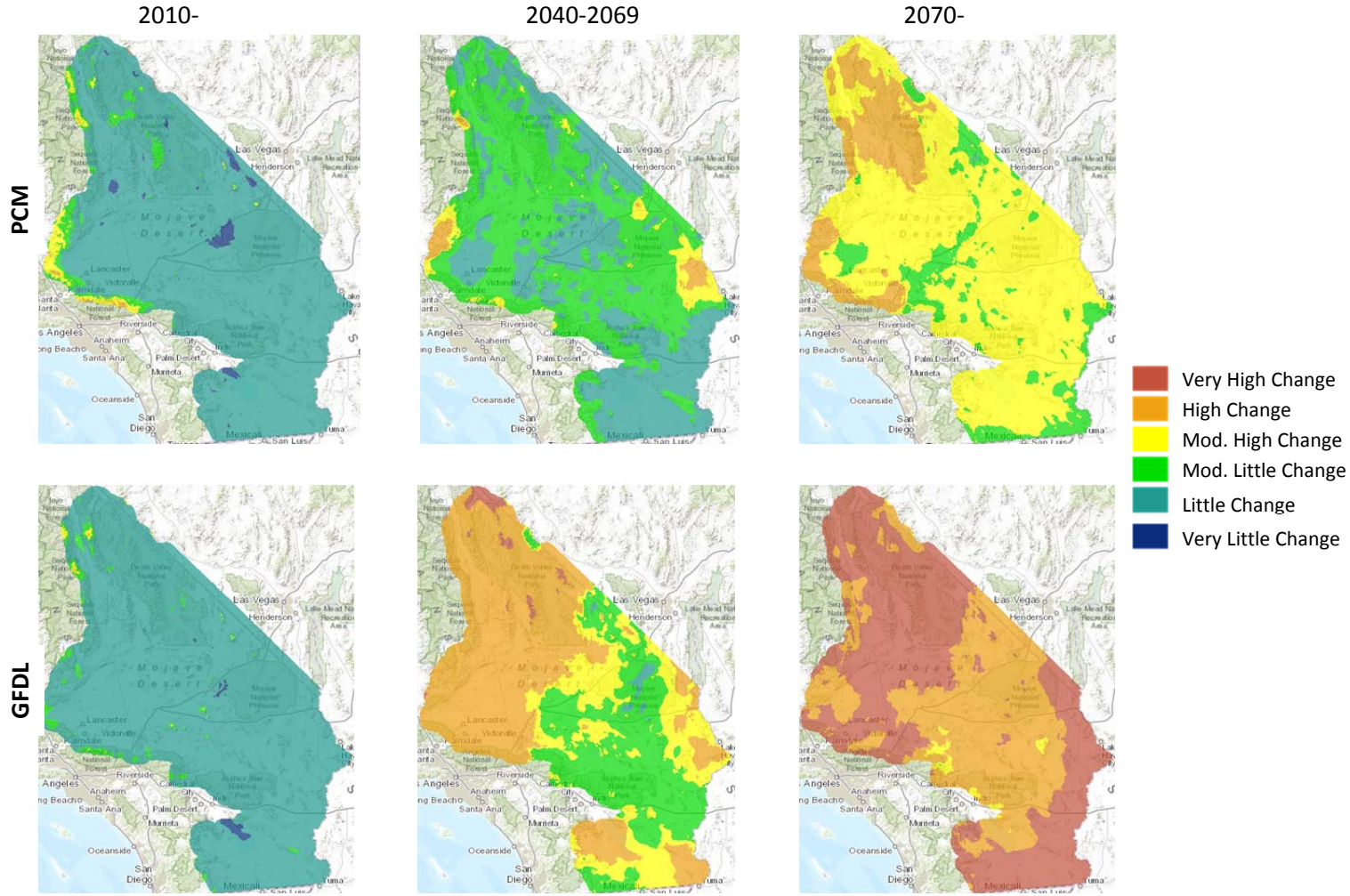

Figure 33. Climate refugia using PCM (top row) and GFDL (bottom row) climate projections under the A2 emission scenario for the DRECP region.

Climate Velocity

Based on the IPCC (2014) summary for policy makers, "Climate velocity is defined as the rate of change in climate over time (e.g., °C/yr, if only temperature is considered) divided by the rate of change in climate over distance (e.g., °C/km, if only temperature is considered) (Loarie et al., 2009; Dobrowski et al., 2013). Climate velocity for temperature is low in mountainous areas because the change in temperature over short distances is large. Climate velocity for temperature is generally high in flat areas because the rate of change in temperature over distance is low. In flat areas, climate velocity can exceed 80 km/yr for the highest rates of projected climate change (RCP 8.5)" (Figure 34). Dobrowski et al. (2013) state that "the use of climate change velocity is considered more biologically relevant (Ackerly et al., 2010) than the use of climate anomalies (*simulated differences between future and current climate*) as it accounts for regional changes in climate and the ability of topographic heterogeneity to buffer biota against these changes".

Because it is expressed in units of distance over time, climate velocity provides a consistent and useful way to compare diverse measures of climate change. Previous analyses of climate change velocity have mostly focused on changes in temperature (e.g. Loarie et al. 2009). In this study, we calculated the climate velocity of a variety of climate variables including aridity, which is defined by UNEP (1992) as the ratio of annual precipitation over annual average potential evapotranspiration.

It seemed unlikely that an area that has already experienced high climate velocity in the past will harbor species with a limited ability to keep up with a similar level of change, unless that it was modest enough for the species to tolerate it or hide from it using local refugia. We therefore decided to calculate the differences between historical and projected maximum climate velocity to provide maps that would show climate stress levels that local species would have or not have experienced historically (Figure 35). For each grid cell, we generated a time series of the velocity for the variable of interest and, for specific periods of time including historical (1971-2000) and futures (2010-2039, 2040-2069, and 2070-2099), we picked the maximum velocity value. We then compared future to historical and mapped the differences.

Loarie et al (2009) calculated global climate velocity using a fairly coarse resolution. For such a small area as DRECP, we used a much finer resolution so we could identify local hotspots of climate velocity (low or high). We used the California Basin Characterization Model (BCM) downscaled CMIP3 climate data (Flint and Flint 2012) at 270m resolution for the 21st century using PCM and GFDL projections under the A2 emissions scenario.

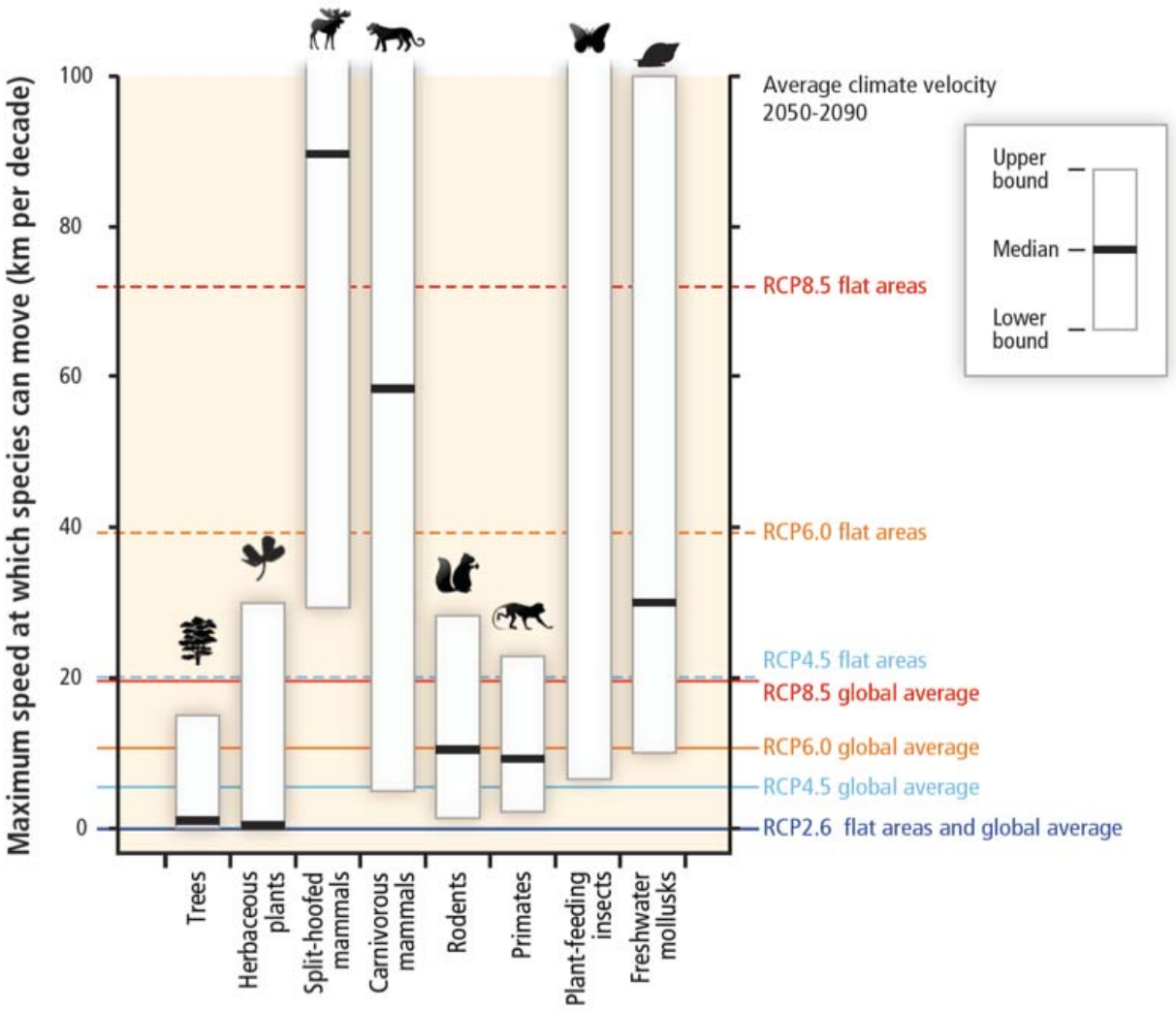

Figure 34 (excerpt from IPCC - Summary to Policy Makers - IPCC 2014). Maximum speeds at which species can move across landscapes (based on observations and models; vertical axis on left), compared with speeds at which temperatures are projected to move across landscapes (climate velocities for temperature; vertical axis on right). White boxes with black bars indicate ranges and medians of maximum movement speeds for trees, plants, mammals, plant-feeding insects (median not estimated), and freshwater mollusks. For RCP2.6, 4.5, 6.0, and 8.5 for 2050-2090, horizontal lines show climate velocity for the global-land-area average and for large flat regions. Species with maximum speeds below each line are expected to be unable to track warming in the absence of human intervention.

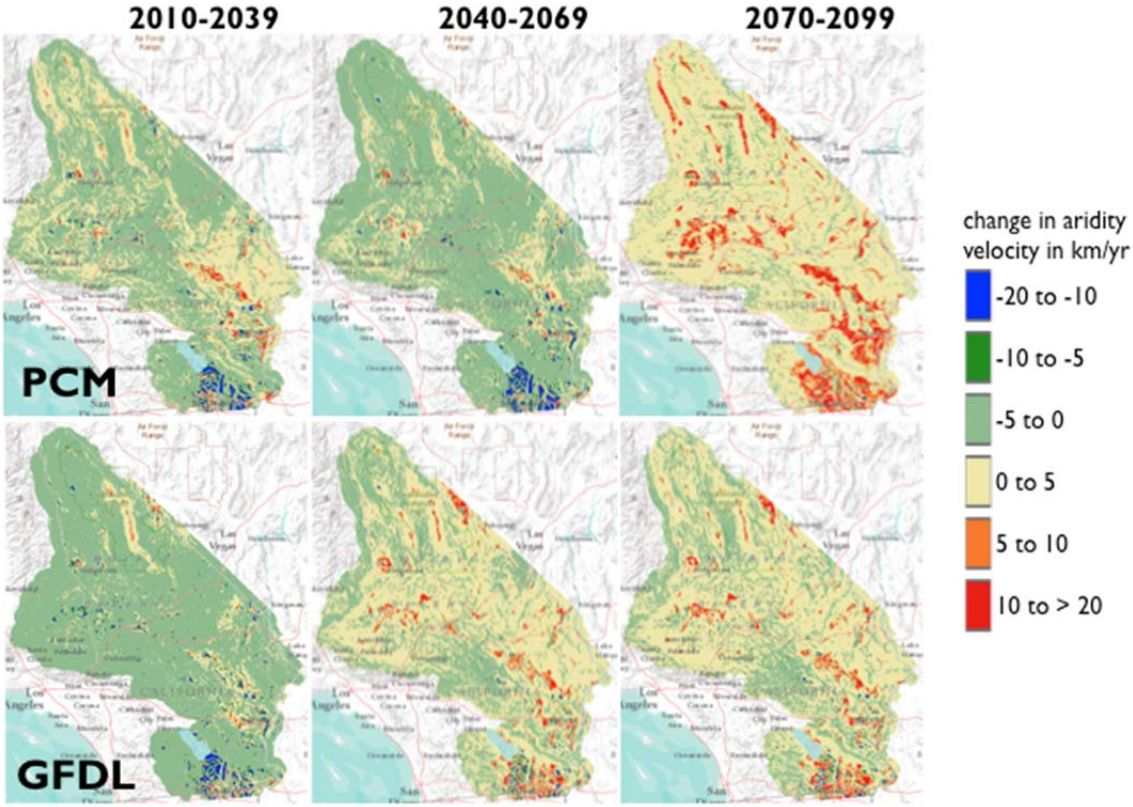

Figure 35. Change in the maximum climate velocity levels for aridity over the DRECP area under the A2 emission scenario in comparison with historical conditions (1971-2000). Climate futures from two GCMs - PCM (top row) and GFDL (bottom row) were provided and downscaled by the California Basin Characterization Model at 270m for three time periods 2010-2039, 2040-2069, and 2070-2099. Note that we capped velocity values at 20km/yr. Red areas will be experiencing greater maximum levels of aridity than they have experienced in the past. On the other hand, in the blue areas, the maximum velocity in aridity will not exceed those maximum levels those areas have experienced in the past.

In the DRECP region (Figure 35), the maps of maximum velocity difference between historical and future conditions clearly show areas in the Sonoran section where aridity levels will exceed anything local plants and animals have experienced in the past. Note that under PCM, maximum velocity is greater in the first part of the 21st century than in the 2050s. This relief however will be short-lived as PCM simulates extreme velocities in the latter part of the century. For GFDL, change in velocity of aridity is noted by mid-century and continues to late-century, but not to the same degree as the PCM model results.

Issue of Scale and Uncertainty with Climate Data and Associated Models

GCMs were originally designed to simulate the earth's climate. Consequently their spatial resolution is coarse. Over time it dropped from the original ~500 km in the early 1990s to ~100 km in 2014 but remained too coarse to be used for local assessments. Even the finer scale of regional climate models (RCMs) (15-50km) are not run at scales of interest for managers. A variety of downscaling methods has been used to provide finer scale climate information (Wilby and Wigley 1998, Díez et al. 2005). The earliest statistical delta or anomaly method uses the difference (or ratio for precipitation) between future and current GCM results, the anomaly or delta, to modify a "baseline" of observed long-term average climate (30 year average). It is important to remember when using downscaled climate that, despite the fact that the information is now served at fine scale, the original information was generated at coarse scale and did not take into account local topography or landcover patchiness and simply assumed homogeneous each grid cell.

A more sophisticated statistical downscaling method corrects the bias that may exist between climate model hindcasts of historical conditions and observations. Future projections are created assuming the bias will remain stable in the future. The most sophisticated downscaling method is dynamic and uses a nested regional climate model (RCM) running at a fine spatial scale but driven by boundary conditions provided by a GCM. RCMs incorporate local topography and more accurate landcover but they still carry any bias that may exist in the GCM that provides its global climate context.

Climate model skill depends foremost on the availability of meteorological data. Ideally, weather stations should be distributed evenly across the landscape so that data interpolation between stations can provide reliable coverage comparable to model results. Unfortunately, the network of meteorological stations can be sparse where population density is low such as in the DRECP region, more stations are usually located in valleys than on ridge tops, in easily accessible sites than in remote areas. As a result, landscape heterogeneity may not be captured by the sparse network and will affect the reliability of climate model projections. When data are scarce, models trained on such data are less likely to produce robust simulations of current conditions, let alone project realistic futures.

Another source of uncertainty results from the lack of fine-scale water features in the climate models. Because most climate models use coarse resolutions, smaller inland water bodies (small streams and ponds) are not included and therefore the local microclimates they help create are not simulated. As a result, fine scale information that includes these

features is important to identify refugia sites that may provide climate buffering opportunities.

In all spatial modeling, scale and resolution matters and working at multiple scales is often required to yield the best outcomes. To illustrate this point, we compared images of a small section of the DRECP region at three spatial resolutions (Figure 36). First, we looked at 30m Digital Elevation Model (DEM) (Figure 36A) where local valleys and ridge tops can easily be identified around the local stream network. We then looked at climate data downscaled to 270m resolution (Flint and Flint 2012) showing less detailed landscape features but still with a reasonable amount of local climate variations visible around the same local stream network (Figure 36B). Finally, we looked at historical climate data provided by the PRISM group (Oregon State University) at 30arc sec. resolution (~800m) (Figure 36C) including the same stream network. It becomes obvious that the last resolution would be best used to explore regional climate patterns over much larger areas. In summary, to interpret and compare the various results from published or state-of-the-art model results available for the DRECP area, spatial scales/resolutions of the information layers need to be taken into account and the applicability of the projections carefully gaged for different land management and planning issues.

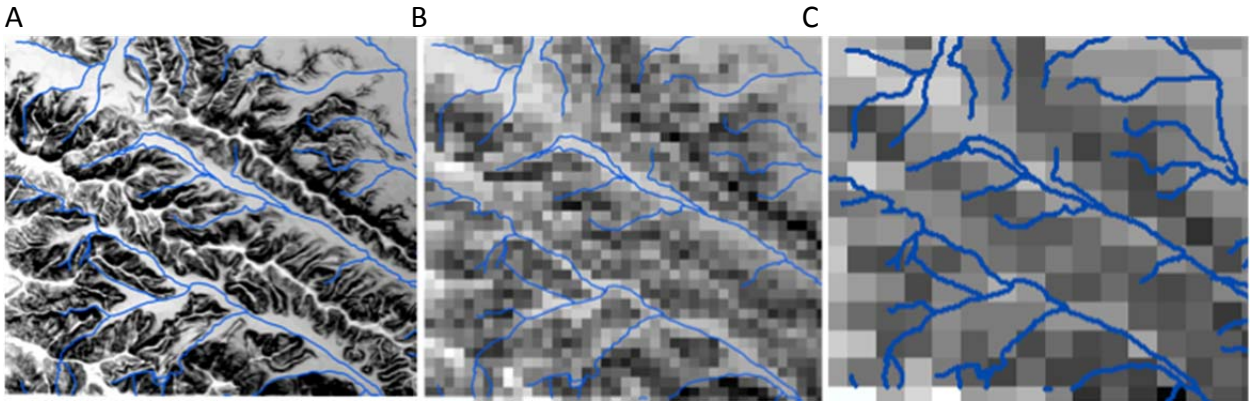

Figure 36. A 30mx30m digital elevation model (A), 270mx270m climate data (Flint and Flint 2012) downscaled from the original PRISM 4km climate (B), and ~800mx800m (30arc sec.) scale original climate data from PRISM (C).

Literature Cited

Abatzoglou J. T. 2012. Development of gridded surface meteorological data for ecological applications and modeling. International Journal of Climatology. doi: 10.1002/joc.3413

Abatzoglou J.T. and T.J. Brown. 2011. A comparison of statistical downscaling methods suited for wildfire applications " Internation Journal of Climatology doi: 10.1002/joc.2312

Alley, R. B., et al. 2007. Summary for policymakers, in Climate Change 2007: The Physical Science Basis. Contribution of Working Group I to the Fourth Assessment Report of the Intergovernmental Panel on Climate Change, edited by S. Solomon et al., pp. 1–18, Cambridge Univ. Press, Cambridge, U. K.

Bachelet D., R.P. Neilson, J. M. Lenihan, and R.J. Drapek. century (Figure 16 and 20). CCSM4 projections show similar magnitude of precipitation compared to historical with a shift toward higher winter contributions (Figure 16 and 20). Climate change effects on vegetation distribution and carbon budget in the U.S. Ecosystems 4:164-185.

Bachelet D., J. Lenihan, R. Drapek, and R. Neilson. century (Figure 16 and 20). CCSM4 projections show similar magnitude of precipitation compared to historical with a shift toward higher winter contributions (Figure 16 and 20). VEMAP vs VINCERA: A DGVM sensitivity to differences in climate scenarios. Global and Planetary Change 64(1-2):38-48.

Bailey, R. G. 1983. Delineation of ecosystem regions. Environmental Management 7: 365-373.

Bell, J. L., L. C. Sloan, and M. A. Snyder. 2004. Regional changes in extreme climatic events: A future climate scenario. Journal of Climate 17:81-87.

Brooks M. L., C. M. D'Antonio, D. M. Richardson, J. B. Grace, J. E. Keeley, J. M. DiTomaso, R. J. Hobbs, M. Pellant, and D. Pyke 2004. Effects of invasive alien plants on fire regimes. BioScience 54: 677-688.

Burke, R.L., M.A. Ewert, J.B. McLemore, and D.R. Jackson. 1996. Temperature-dependent sex determination and hatching success in the gopher tortoise (*Gopherus polyphemus*). Chelonian Conservation and Biology 2(1):86-88.

Cayan, D.R., E.P. Maurer, M.D. Dettinger, M. Tyree, and K. Hayhoe. 2008. Climate change scenarios for California region. Climate Change (2008)87(Suppl 1):S21-S42 DOI 10.1007/s10584-007-9377-6.

Christensen, N. S., and D. P. Lettenmaier. 2007. A multimodel ensemble approach to assessment of climate change impacts on the hydrology and water resources of the Colorado River Basin. Hydrology and Earth System Sciences 11:1417-1434.

D'Antonio, C. M. and P. M. Vitousek. 1992. Biological invasions by exotic grasses, the grass/fire cycle, and global change. Annual Review of Ecology and Systematics 23:63–87.

Daly, C., M. Halbleib, J. I. Smith, W. P. Gibson, M. K. Doggett, G. H. Taylor, J. Curtis, and P. P. Pasteris. 2008. Physiographically sensitive mapping of climatological temperature and precipitation across the conterminous United States, Int. J. Climatol. 28(15):2031–2064, doi:10.1002/joc.1688.

Díez, E., C. Primo, J. A. García-Moya, J. M. Gutiérrez and B. Orfila. 2005. Statistical and dynamical downscaling of precipitation over Spain from DEMETER seasonal forecasts. Tellus 57A: 409-423.

Dobrowski, S.Z., J. Abatzoglou, A.K. Swanson, J.A. Greenberg, A.R. Mynsberge, Z.A. Holden, Z.A., and M.K. Schwartz. 2013. The climate velocity of the contiguous United States during the 20th century. Global Change Biology 19(1):241-251.

Ficklin D.L., I.T. Stewart, and E.P. Maurer. 2013. Climate Change Impacts on Streamflow and Subbasin-Scale Hydrology in the Upper Colorado River Basin. PLoS ONE 8(8): e71297. doi:10.1371/journal.pone.0071297

Flint, L.E. and A.L. Flint. 2012. Downscaling future climate scenarios to fine scales for hydrologic and ecological modeling and analysis. Ecological Processes 1:1 http:/www.ecological processes.com/1/1/2.

Geil, K. L., Y. L. Serra and X. Zeng. 2014. Assessment of CMIP5 Model Simulation of the North American Monsoon System. J. Climate 26(22): 8787–8801.

Guida, R.J. 2011. Climate and vegetation change in the Newberry mountains, Southern Clark County, Nevada. *UNLV Theses/Dissertations/Professional Papers/Capstones.* Paper 1232. 120pp.

Harding B.L., A.W. Wood, and J.R. Prairie. 2012. The implications of climate change scenario selection for future streamflow projection in the Upper Colorado River Basin. Hydrol Earth Syst Sci Discuss 16: 3989–4007.

Hunt, C.B. 1975. Death Valley: Geology, Ecology, Archaeology. University of California Press, Berkeley, California. 234pp.

IPCC, 2014: Summary for policymakers. In: Climate Change 2014: Impacts, Adaptation, and Vulnerability. Part A: Global and Sectoral Aspects. Contribution of Working Group II to the Fifth Assessment Report of the Intergovernmental Panel on Climate Change [Field,

C.B., V.R. Barros, D.J. Dokken, K.J. Mach, M.D. Mastrandrea, T.E. Bilir, M. Chatterjee, K.L. Ebi, Y.O. Estrada, R.C. Genova, B. Girma, E.S. Kissel, A.N. Levy, S. MacCracken, P.R. Mastrandrea, and L.L. White (eds.)]. Cambridge University Press, Cambridge, United Kingdom and New York, NY, USA, pp. 1-32.

Jevrejeva, S., J.C. Moore, and A. Grinsted. 2012. Saa level projections to AD2500 with a new generation of climate change scenarios. Global and Planetary Change 80-81:14-20.

Kelly, A.E. and M.L. Goulden. 2008. Rapid shifts in plant distribution with recent climate change. Proc. Natl. Acad. Sci. U.S.A. 105, 11823–11826.

LaDochy, S., R. Medina, and W. Patzert. 2007. Recent California climate variability: spatial and temporal patterns in temperature trends. Clim. Res. 33: 159–169.

Lenihan, J. M., D. Bachelet, R. P. Neilson, and R. Drapek. 2008. Response of vegetation distribution, ecosystem productivity, and fire to climate change scenarios for California. Climatic Change 87:S215-S230.

Loarie, S.R., B.E. Carter, K. Hayhoe, Sean McMahon, R. Moe, C.A. Knight, and D. Ackerly . 2009. Climate change and the future of California's endemic flora. PLOS ONE 3(6): e2502. DOI: 10.1371/journal.pne.0002502.

MacMahon, J.A. 2000. Warm Deserts, Chapter 8. pp. 285-322. In: Barbour and Billings (eds) North American Terrestrial Vegetation, 2nd edition. pp. 285-322.

McMahon, J.A. and F.H. Wagner. 1985. The Mohave, Sonoran and Chihuahuan Deserts of North America. In: M. Evenari, I. Noy-Meir, and D.W. Goodall (eds). Hot deserts and arid shrublands. A. Ecosystems of the World, Vol. 12A. Elsevier, Amsterdam.

Moritz, M.A., M-A. Parisien, E. Batllori, M. A. Krawchuk, J. Van Dorn, D. J. Ganz, and K. Hayhoe. 2012. Climate change and disruptions to global fire activity. Ecosphere 3:art49. http://dx.doi.org/10.1890/ES11-00345.1

Moss, R.H., M. Babiker, S. Brinkman, E. Calvo, T. Carter, J. Edmonds, I. Elgizouli, S. Emori, L. Erda, K. Hibbard, R. Jones, M. Kainuma, J. Kelleher, J.F. Lamarque, M. Manning, B. Matthews, J. Meehl, L. Meyer, J. Mitchell, N. Nakicenovic, B. O'Neill, R. Pichs, K. Riahi, S. Rose, P. Runci, R. Stouffer, D. van Vuuren, J. Weyant, T. Wilbanks, J.P. van Ypersele, and M. Zurek. 2008. Towards New Scenarios for Analysis of Emissions, Climate Change, Impacts, and Response Strategies. Intergovernmental Panel on Climate Change, Geneva, 132 pp.

Moss, R.H., J.A. Edmonds, K.A. Hibbard, K.A., Manning, M.R., Rose, S.K., van Vuuren, D.P., Carter, T.R., Emori, S., Kainuma, M., Kram, T., Meehl, G.A., Mitchell, J.F., Nakicenovic, N., Riahi, K., Smith, S.J., Stouffer, R.J., Thomson, A.M., Weyant, J.P., Wilbanks, T.J. 2010. The next generation of scenarios for climate change research and assessment. Nature 463(7282):747-56.

Nakicenovic, N., J. Alcamo, G. Davis, B. de Vries, J. Fenhann, S. Gaffin, K. Gregory, A. Grübler, T. Y. Jung, T. Kram, E. Lebre La Rovere, L. Michaelis, S. Mori, T. Morita, W. Pepper, H. Pitcher, L. Price, K. Riahi, A. Roehrl, H-H Rogner, A. Sankovski, M. Schlesinger, P. Shukla, S. Smith, R. Swart, S. van Rooijen, N. Victor, and Z. Dadi. 2000. Special Report on Emissions Scenarios: A Special Report of Working Group III of the Intergovernmental Panel on Climate Change. Cambridge University Press, Cambridge, U.K. 599 pp. Available online at: http://www.grida.no/climate/ipcc/emission/index.htm

Neelin, J. D., B. Langenbrunner, J. E. Meyerson, A. Hall, and N. Berg. 2013. California winter precipitation change under global warming in the Coupled Model Intercomparison Project 5 ensemble. J. Climate 26:6238-6256, doi:10.1175/JCLI-D-12-00514.1.

Omernik, J.M. 1987. Ecoregions of the conterminous United States. Map (scale 1:7,500,000). Annals of the Association of American Geographers 77(1):118-125.

Parry, M., O. Canziani, J. Palutikof, P. van der Linden, and C.E. Hanson (eds). 2007. Climate Change 2007: Impacts, Adaptation, and Vulnerability. Contribution of Working Group II to the Fourth Assessment Report of the Intergovernmental Panel on Climate Change (IPCC). Cambridge University Press, Cambridge, United Kingdom, 976pp.

PRBO Conservation Science. 2011. Projected effects of climate change in California: Ecoregional summaries emphasizing consequences for wildlife. Version 1.0. http://data.prbo.org/apps/bssc/uploads/Ecoregional021011.pdf

Rogelj, J., M. Meinhausen, and R. Knutti. 2012. Global warming under old and new scenarios using IPCC climate sensitivity range estimates. Nature Climate Change 2: 248-253.

Rupp, D. E., J. T. Abatzoglou, K. C. Hegewisch, and P. W. Mote. 2013. Evaluation of CMIP5 20th century climate simulations for the Pacific Northwest USA, J. Geophys. Res. Atmos., 118, doi:10.1002/jgrd.50843.

Sanford, T., P.C. Frumhoff, A. Luers, and J. Gulledge. 2014. The climate policy narrative for a dangerously warming world. Nature Climate Change 4:164-166.

Snyder, M.A., L.C. Sloan, and J.L. Bell. 2004. Modeled regional climate change in the hydrologic regions of California: A CO_2 sensitivity study. Journal of the American Water Resources Association 40:591-601.

Snyder, M.A. and L.C. Sloan. 2005. Transient future climate over the western United States using a regional climate model. Earth Interactions 9: Article No. 11.

Spotila, J.R., L.C. Zimmerman, C.A. Binckley, J.A. Grumbles, D.C. Rostal, A. List, Jr., E.C. Beyer, K.M. Phillips, and S.J. Kemp. 1994. Effects of incubation conditions on sex

determination, hatching success, and growth of hatchling desert tortoises, *Gopherus agassizii*. Herpetological Monographs 8:103-116.

Stahlschmidt, Z.R., D.F. DeNardo, J.N. Holland, B.P. Kotler, and M. Kruse-Peeples. 2011. Tolerance mechanisms in North American deserts: Biological and societal approaches to climate change. Journal of Arid Environments 75(2011):681-687.

Stralberg, D., D. Jongsomjit, C.A. Howell, M.A. Snyder, J.D. Alexander, J.A. Wiens, T.L. Root. 2009. Re-Shuffling of Species with Climate Disruption: A No-Analog Future for California Birds? PLOS ONE 4(9): e6825. DOI:10.1371/journal.pone.0006825.

UNEP. 1992. World Atlas of Desertification. Edward Arnold. London.

VanVuuren, D., J Edmonds, M. Kainuma, K. Riahi, A. Thomson, K. Hibbard, G.C. Hurtt, T. Kram, V. Krey, J. Lamarque, T. Masui, M. Meinshausen, N. Nakicenovic, S.J. Smith, and S.K. Rose. 2011. The representative concentration pathways: an overview. Climatic Science 109:5-31.

Westerling, A.L., H.G. Hidalgo, D.R. Cayan, and T.W. Swetnam. 2006. Warming and Earlier Spring Increases Western U.S. Forest Wildfire Activity. Science 313: 940-943. DOI:10.1126/science.1128834.

Wilby, R.L., T.M.L. Wigley, D. Conway, P.D. Jones, B.C. Hewitson, J. Main, and D.S. Wilks. 1998. Statistical downscaling of general circulation model output: a comparison of methods. Water Resources Research 34:2995–3008.

Wood, D. A., A. G. Vandergast, K. R. Barr, R. D. Inman, T. C. Esque, K. E. Nussear, and R. N. Fisher. 2012. Comparative phylogeography reveals deep lineages and regional evolutionary hotspots in the Mojave and Sonoran Deserts. Diversity and Distributions DOI: 10.1111/ddi.12022:1-16.

Appendix - Glossary

Anomaly: Difference (or ratio) between a projection and the historical baseline.

Baseline (excerpt from IPCC 2013): The baseline (or reference) is the state against which change is measured. A baseline period is the period relative to which anomalies are computed.

Carbon dioxide (CO2)(excerpt from IPCC 2013): "A naturally occurring gas, also a by-product of burning fossil fuels from fossil carbon deposits, such as oil, gas and coal, of burning biomass, of land use changes and of industrial processes (e.g., cement production). It is the principal anthropogenic greenhouse gas that affects the earth's radiative balance. It is the reference gas against which other greenhouse gases are measured and therefore has a Global Warming Potential of 1."

Carbon dioxide (CO2) fertilization (excerpt from IPCC 2013): "The enhancement of the growth of plants as a result of increased atmospheric carbon dioxide (CO2) concentration."

Climate (excerpt from IPCC 2013): Climate in a narrow sense is usually defined as the average weather, or more rigorously, as the statistical description in terms of the mean and variability of relevant quantities over a period of time ranging from months to thousands or millions of years. The classical period for averaging these variables is 30 years, as defined by the World Meteorological Organization. The relevant quantities are most often surface variables such as temperature, precipitation and wind. Climate in a wider sense is the state, including a statistical description, of the climate system.

Climate change (excerpt from IPCC 2013): "refers to a change in the state of the climate that can be identified (e.g., by using statistical tests) by changes in the mean and/or the variability of its properties, and that persists for an extended period, typically decades or longer. Climate change may be due to natural internal processes or external forcings such as modulations of the solar cycles, volcanic eruptions and persistent anthropogenic changes in the composition of the atmosphere or in land use. Note that the Framework Convention on Climate Change (UNFCCC), in its Article 1, defines climate change as: 'a change of climate which is attributed directly or indirectly to human activity that alters the composition of the global atmosphere and which is in addition to natural climate variability observed over comparable time periods'. The UNFCCC thus makes a distinction between climate change attributable to human activities altering the atmospheric composition, and climate variability attributable to natural causes.

Climate model (excerpt from IPCC 2013): A numerical representation of the climate system based on the physical, chemical and biological properties of its components, their interactions and feedback processes, and accounting for some of its known properties. Coupled Atmosphere–Ocean General Circulation Models (**AOGCMs**) provide a representation of the climate system that is near or at the most comprehensive end of the

spectrum currently available. There is an evolution towards more complex models with interactive chemistry and biology. See **ESMs.**

Climate normals: NOAA's computation of climate Normals is in accordance with the recommendation of the World Meteorological Organization (WMO), of which the United States is a member. While the WMO mandates each member nation to compute 30-year averages of meteorological quantities at least every 30 years (1931 - 1960, 1961 - 1990, 1991 - 2020, etc.), the WMO recommends a decadal update, in part to incorporate newer weather stations. Meteorologists and climatologists regularly use Normals for placing recent climate conditions into a historical context. In addition to weather and climate comparisons, Normals are utilized in seemingly countless applications such as regulation of power companies, energy load forecasting, crop selection and planting times, construction planning, building design, and many others.

Climate prediction (excerpt from IPCC 2013): A climate prediction or climate forecast is the result of an attempt to produce (starting from a particular state of the climate system) an estimate of the actual evolution of the climate in the future, for example, at seasonal, interannual or decadal time scales. Because the future evolution of the climate system may be highly sensitive to initial conditions, such predictions are usually probabilistic in nature.

Climate projection (excerpt from IPCC 2013): A climate projection is the simulated response of the climate system to a scenario of future emission or concentration of greenhouse gases and aerosols, generally derived using climate models. Climate projections are distinguished from climate predictions by their dependence on the emission/concentration/radiative forcing scenario used, which is in turn based on assumptions concerning, for example, future socioeconomic and technological developments that may or may not be realized.

Climate scenario (excerpt from IPCC 2013): A plausible and often simplified representation of the future climate, based on an internally consistent set of climatological relationships that has been constructed for explicit use in investigating the potential consequences of anthropogenic climate change, often serving as input to impact models. Climate projections often serve as the raw material for constructing climate scenarios, but climate scenarios usually require additional information such as the observed current climate. A climate change scenario is the difference between a climate scenario and the current climate.

Climate system (excerpt from IPCC 2013): The climate system is the highly complex system consisting of five major components: the atmosphere, the hydrosphere, the cryosphere, the lithosphere and the biosphere, and the interactions between them. The climate system evolves in time under the influence of its own internal dynamics and because of external forcings such as volcanic eruptions, solar variations and anthropogenic forcings such as the changing composition of the atmosphere and land use change.

Climate velocity: measure of the velocity over the ground, in a particular location and in a potentially changing climate, which would be necessary to maintain a constant value for a particular measure of climate. For instance, in a warming climate, an organism might be able to maintain a constant temperature by moving uphill; the speed and direction, which would be needed to maintain a constant temperature would be the climate velocity with respect to temperature.

Downscaling (excerpt from IPCC 2013): Downscaling is a method that derives local- to regional- scale (10 to 100 km) information from larger-scale models or data analyses. Two main methods exist: dynamical downscaling and empirical/statistical downscaling. The dynamical method uses the output of regional climate models, global models with variable spatial resolution or high-resolution global models. The empirical/statistical methods develop statistical relationships that link the large-scale atmospheric variables with local/regional climate variables. In all cases, the quality of the driving model remains an important limitation on the quality of the downscaled information.

Drought (excerpt from IPCC 2013): A period of abnormally dry weather long enough to cause a serious hydrological imbalance. Drought is a relative term; therefore any discussion in terms of precipitation deficit must refer to the particular precipitation-related activity that is under discussion. For example, shortage of precipitation during the growing season impinges on crop production or ecosystem function in general (due to soil moisture drought, also termed agricultural drought), and during the runoff and percolation season primarily affects water supplies (hydrological drought). Storage changes in soil moisture and groundwater are also affected by increases in actual evapotranspiration in addition to reductions in precipitation. A period with an abnormal precipitation deficit is defined as a meteorological drought. A megadrought is a very lengthy and pervasive drought, lasting much longer than normal, usually a decade or more.

Earth System Model (**ESM**) (excerpt from IPCC 2013): A coupled atmosphere–ocean general circulation model in which a representation of the carbon cycle is included, allowing for interactive calculation of atmospheric CO2 or compatible emissions. Additional components (e.g., atmospheric chemistry, ice sheets, dynamic vegetation, nitrogen cycle, but also urban or crop models) may be included.

Emission scenario (excerpt from IPCC 2013): A plausible representation of the future development of emissions of substances that are potentially radiatively active (e.g., greenhouse gases, aerosols) based on a coherent and internally consistent set of assumptions about driving forces (such as demographic and socioeconomic development, technological change) and their key relationships. Concentration scenarios, derived from emission scenarios, are used as input to a climate model to compute climate projections. In IPCC (1992) a set of emission scenarios was presented which were used as a basis for the climate projections in IPCC (1996). These emission scenarios are referred to as the IS92 scenarios. In the IPCC Special Report on Emission Scenarios (Nakićenović et al. 2000) emission scenarios, the so-called SRES scenarios, were published, some of which were used, among others, as a basis for the climate projections presented in Chapters 9 to 11 of IPCC (2001) and Chapters 10 and 11 of IPCC (2007). New emission scenarios for climate

change, the four Representative Concentration Pathways, were developed for, but independently of, the present IPCC assessment.

Equivalent carbon dioxide (CO_2) concentration (excerpt from IPCC 2013): The concentration of carbon dioxide that would cause the same radiative forcing as a given mixture of carbon dioxide and other forcing components. Those values may consider only greenhouse gases, or a combination of greenhouse gases and aerosols. Equivalent carbon dioxide concentration is a metric for comparing radiative forcing of a mix of different greenhouse gases at a particular time but does not imply equivalence of the corresponding climate change responses nor future forcing. There is generally no connection between equivalent carbon dioxide emissions and resulting equivalent carbon dioxide concentrations.

Equivalent carbon dioxide (CO_2) emission (excerpt from IPCC 2013): The amount of carbon dioxide emission that would cause the same integrated radiative forcing, over a given time horizon, as an emitted amount of a greenhouse gas or a mixture of greenhouse gases. The equivalent carbon dioxide emission is obtained by multiplying the emission of a greenhouse gas by its Global Warming Potential for the given time horizon. For a mix of greenhouse gases it is obtained by summing the equivalent carbon dioxide emissions of each gas. Equivalent carbon dioxide emission is a common scale for comparing emissions of different greenhouse gases but does not imply equivalence of the corresponding climate change responses.

Extreme weather event (excerpt from IPCC 2013): An extreme weather event is an event that is rare at a particular place and time of year. By definition, the characteristics of what is called extreme weather may vary from place to place in an absolute sense. When a pattern of extreme weather persists for some time, such as a season, it may be classed as an extreme climate event, especially if it yields an average or total that is itself extreme (e.g., drought or heavy rainfall over a season).

General circulation (excerpt from IPCC 2013): The large-scale motions of the atmosphere and the ocean as a consequence of differential heating on a rotating Earth. General circulation contributes to the energy balance of the system through transport of heat and momentum.

General Circulation Model (GCM) - see climate model

Greenhouse effect (excerpt from IPCC 2013): The infrared radiative effect of all infrared-absorbing constituents in the atmosphere. Greenhouse gases, clouds, and (to a small extent) aerosols absorb terrestrial radiation emitted by the earth's surface and elsewhere in the atmosphere. These substances emit infrared radiation in all directions, but, everything else being equal, the net amount emitted to space is normally less than would have been emitted in the absence of these absorbers because of the decline of temperature with altitude in the troposphere and the consequent weakening of emission. An increase in the concentration of greenhouse gases increases the magnitude of this effect; the difference is sometimes called the enhanced greenhouse effect. The change in a greenhouse gas

concentration because of anthropogenic emissions contributes to an instantaneous radiative forcing. Surface temperature and troposphere warm in response to this forcing, gradually restoring the radiative balance at the top of the atmosphere.

Greenhouse gas (GHG) (excerpt from IPCC 2013): Greenhouse gases are those gaseous constituents of the atmosphere, both natural and anthropogenic, that absorb and emit radiation at specific wavelengths within the spectrum of terrestrial radiation emitted by the earth's surface, the atmosphere itself, and by clouds. This property causes the greenhouse effect. Water vapor (H2O), carbon dioxide (CO2), nitrous oxide (N2O), methane (CH4) and ozone (O3) are the primary greenhouse gases in the earth's atmosphere. Moreover, there are a number of entirely human-made greenhouse gases in the atmosphere, such as the halocarbons and other chlorine- and bromine- containing substances, dealt with under the Montreal Protocol. Beside CO_2, N_2O and CH_4, the Kyoto Protocol deals with the greenhouse gases sulphur hexafluoride (SF6), hydrofluorocarbons (HFCs) and perfluorocarbons (PFCs).

Land use and Land use change (excerpt from IPCC 2013): Land use refers to the total of arrangements, activities and inputs undertaken in a certain land cover type (a set of human actions). The term land use is also used in the sense of the social and economic purposes for which land is managed (e.g., grazing, timber extraction and conservation). Land use change refers to a change in the use or management of land by humans, which may lead to a change in land cover. Land cover and land use change may have an impact on the surface albedo, evapotranspiration, sources and sinks of greenhouse gases, or other properties of the climate system and may thus give rise to radiative forcing and/or other impacts on climate, locally or globally.

MACA: Multivariate Adaptive Constructed Analogues (Abatzoglou 2012). MACA is a statistical method for downscaling Global Climate Models (GCMs) from their native coarse resolution to a higher spatial resolution that captures both the scales relevant for impact modeling while preserving time-scales and patterns of meteorology as simulated by GCMs. This method has been shown to be slightly preferable to direct daily interpolated bias correction in regions of complex terrain due to its use of a historical library of observations and multivariate approach (Abatzoglou and Brown, 2011). Variables that are downscaled include 2-m maximum/minimum temperature, 2-m maximum/minimum relative humidity, 10-m zonal and meridional wind, downward shortwave radiation at the surface, 2-m specific humidity, and precipitation accumulation all at the daily timestep. http://maca.northwestknowledge.net/

Monsoon (excerpt from IPCC 2013): A monsoon is a tropical and subtropical seasonal reversal in both the surface winds and associated precipitation, caused by differential heating between a continental-scale land mass and the adjacent ocean. Monsoon rains occur mainly over land in summer.

Nonlinearity (excerpt from IPCC 2013): A process is called nonlinear when there is no simple proportional relation between cause and effect. Climate and biological systems

contain many such nonlinear processes, resulting in a system with potentially very complex behavior. Such complexity may lead to tipping points.

Predictability (excerpt from IPCC 2013): The extent to which future states of a system may be predicted based on knowledge of current and past states of the system. Because knowledge of the climate system's past and current states is generally imperfect, as are the models that utilize this knowledge to produce a climate prediction, and because the climate system is inherently nonlinear and chaotic, predictability of the climate system is inherently limited. Even with arbitrarily accurate models and observations, there may still be limits to the predictability of such a nonlinear system (AMS, 2000).

Process-based model (excerpt from IPCC 2013): Theoretical concepts and computational methods that represent and simulate the behavior of real-world systems derived from a set of functional components and their interactions with each other and the system environment, through physical and mechanistic processes occurring over time.

Radiative forcing (excerpt from IPCC 2013): Radiative forcing is the change in the net, downward minus upward, radiative flux (expressed in W m–2) at the tropopause or top of atmosphere due to a change in an external driver of climate change, such as, for example, a change in the concentration of carbon dioxide or the output of the Sun. Sometimes internal drivers are still treated as forcings even though they result from the alteration in climate, for example aerosol or greenhouse gas changes in paleoclimates. The traditional radiative forcing is computed with all tropospheric properties held fixed at their unperturbed values, and after allowing for stratospheric temperatures, if perturbed, to readjust to radiative-dynamical equilibrium. Radiative forcing is called instantaneous if no change in stratospheric temperature is accounted for. The radiative forcing once rapid adjustments are accounted for is termed the effective radiative forcing. Radiative forcing is not to be confused with cloud radiative forcing, which describes an unrelated measure of the impact of clouds on the radiative flux at the top of the atmosphere.

Regional Climate Model (RCM) (excerpt from IPCC 2013): A climate model at higher resolution over a limited area. Such models are used in downscaling global climate results over specific regional domains.

Representative Concentration Pathways (RCPs) (excerpt from IPCC 2013): Scenarios that include time series of emissions and concentrations of the full suite of greenhouse gases and aerosols and chemically active gases, as well as land use/land cover (Moss et al., 2008). The word **representative** signifies that each RCP provides only one of many possible scenarios that would lead to the specific radiative forcing characteristics. The term **pathway** emphasizes that not only the long-term concentration levels are of interest, but also the trajectory taken over time to reach that outcome. (Moss et al., 2010).
Four RCPs produced from Integrated Assessment Models were selected from the published literature and are used in the present IPCC Assessment as a basis for the climate predictions and projections:

RCP2.6 - One pathway where radiative forcing peaks at approximately 3 W m–2 before 2100 and then declines.

RCP4.5 and RCP6.0 - Two intermediate stabilization pathways in which radiative forcing is stabilized at approximately 4.5 W m–2 and 6.0 W m–2 after 2100.
RCP8.5 - One high pathway for which radiative forcing reaches greater than 8.5 W m–2 by 2100 and continues to rise for some amount of time.

Runoff (excerpt from IPCC 2013): That part of precipitation that does not evaporate and is not transpired, but flows through the ground or over the ground surface and returns to bodies of water.

Scenario (excerpt from IPCC 2013): A plausible description of how the future may develop based on a coherent and internally consistent set of assumptions about key driving forces (e.g., rate of technological change, prices) and relationships. Note that scenarios are neither predictions nor forecasts, but are useful to provide a view of the implications of developments and actions.

Smoothing kernel: discrete approximation of a smoothing function which is typically applied via a convolution operation to filter out high (spatial) frequency components of a multi-dimensional discrete signal. Since the derivative is definable only where the signal is smooth, we must smooth the signal before calculating the derivative.

Sobel operator: matrix operation used for efficiently approximating the derivative (gradient) of a multi-dimensional discrete signal.

Snow water equivalent (SWE) (excerpt from IPCC 2013): The depth of liquid water that would result if a mass of snow melted completely.

Soil moisture (excerpt from IPCC 2013): Water stored in the soil in liquid or frozen form.

Soil temperature (excerpt from IPCC 2013): The temperature of the soil. This can be measured or modelled at multiple levels within the depth of the soil.

Spatial and temporal scales (excerpt from IPCC 2013): Spatial scales may range from local (less than 100 000 km^2), through regional (100 000 to 10 million km^2) to continental (10 to 100 million km^2). Temporal scales may range from seasonal to geological (up to hundreds of millions of years).

SRES scenarios (excerpt from IPCC 2013): "emission scenarios developed by Nakićenović et al. (2000) and used, among others, as a basis for some of the climate projections shown in Chapters 9 to 11 of IPCC (2001) and Chapters 10 and 11 of IPCC (2007). The following terms are relevant for a better understanding of the structure and use of the set of SRES scenarios:

Scenario family: Scenarios that have a similar demographic, societal, economic and technical change storyline.
Four scenario families comprise the SRES scenario set: **A1, A2, B1** and **B2**.

Storyline: A narrative description of a scenario (or family of scenarios), highlighting the main scenario characteristics, relationships between key driving forces and the dynamics of their evolution.

Streamflow (excerpt from IPCC 2013): Water flow within a river channel, for example expressed in $m^3\ s^{-1}$. A synonym for river discharge.

Tipping point (excerpt from IPCC 2013): "In climate, a hypothesized critical threshold when global or regional climate changes from one stable state to another stable state. The tipping point event may be irreversible."

Uncertainty (excerpt fro, IPCC 2013): "A state of incomplete knowledge that can result from a lack of information or from disagreement about what is known or even knowable. It may have many types of sources, from imprecision in the data to ambiguously defined concepts or terminology, or uncertain projections of human behavior. Uncertainty can therefore be represented by quantitative measures (e.g., a probability density function) or by qualitative statements (e.g., reflecting the judgment of a team of experts). "